Check for updates

ADVANCED FUNCTIONAL MATERIALS
www.afm-journal.de

Smarter Sensors Through Machine Learning: Historical Insights and Emerging Trends across Sensor Technologies

Kichul Lee, Osman Gul, Yeongjae Kwon, Jaeseok Jeong, Seokjoo Cho, Jihyeon Ahn, Jehee Yu, Cheolmin Kim, Donho Lee, Hyeonseok Han, Byeongju Lee, Jungrak Choi, Ji-Hwan Ha, Yongrok Jeong, Kyungnam Kang, Ali Javey, Junseong Ahn,* and Inkyu Park**

In the evolving landscape of the Internet of Things (IoT), the deployment of sensors is surging, along with increasing demands for higher performance. However, improving sensor capabilities solely through hardware advancements, such as material and structural design, faces inherent limitations. Common sensing materials, including semiconducting metal oxides, graphene, conductive polymers, elastomers, and noble metals, suffer from issues such as poor selectivity, slow response time, and low resolution, which hinder their practical applications. To address these challenges, recent efforts focus on leveraging machine learning (ML) for sensor signal processing, enhancing performance beyond conventional hardware-based approaches. This review explores the role of ML in advancing next-generation physical and chemical sensors. It examines how ML-driven signal processing enhances key sensor attributes, such as selectivity, response time, spatial resolution, stability, power consumption, and analysis process. Additionally, widely adopted ML techniques are systematically categorized based on their targeted performance improvements, and promising strategies to overcome existing bottlenecks are discussed. The review also highlights potential applications of ML-enhanced sensors, providing insights into their commercialization prospects. By presenting a structured analysis and future outlook, this paper aims to support the continued integration of ML into sensor technology and inspire further research in this rapidly evolving field.

1. Introduction

As society transitions into the era of the Internet of Things (IoT), the demand for sensors has surged, not only in quantity but also in complexity and performance requirements.[1–6] These sensors must function reliably in diverse and challenging environments, supporting applications such as augmented and virtual reality (AR/VR) systems, smart factories, personalized healthcare, and precision agriculture.[7–19] To meet these evolving demands, researchers are focusing on developing soft, compact, and multifunctional sensors that surpass the capabilities of conventional sensor technologies.[20–47] However, improving sensor performance solely through hardware advancements, such as novel material development and structural optimization, has fundamental limitations. Intrinsic shortcomings of widely used sensing materials further hinder sensor performance. For instance, chemical sensors, particularly those based on chemiresistive mechanisms, generally suffer from low

K. Lee, O. Gul, Y. Kwon, J. Jeong, S. Cho, J. Ahn, J. Yu, C. Kim, D. Lee, H. Han, B. Lee, I. Park
Department of Mechanical Engineering
KAIST
Daejeon 34141, Republic of Korea
E-mail: inkyu@kaist.ac.kr

B. Lee, J. Choi, K. Kang
Electronics and Telecommunications Research Institute (ETRI)
Daejeon 34129, Republic of Korea

The ORCID identification number(s) for the author(s) of this article can be found under https://doi.org/10.1002/adfm.202519859

© 2025 The Author(s). Advanced Functional Materials published by Wiley-VCH GmbH. This is an open access article under the terms of the Creative Commons Attribution-NonCommercial License, which permits use, distribution and reproduction in any medium, provided the original work is properly cited and is not used for commercial purposes.

DOI: 10.1002/adfm.202519859

J.-H. Ha
Department of Mechanical Engineering
Hanbat National University
Daejeon 34158, Republic of Korea

Y. Jeong
School of Mechanical Engineering
Kyungpook National University
Daegu 41566, South Korea

K. Lee, A. Javey
Department of Electrical Engineering and Computer Sciences
University of California
Berkeley, CA 94720, USA
E-mail: ajavey@berkeley.edu

J. Ahn
Department of Control and Instrumentation Engineering
Korea University
Sejong 30019, Republic of Korea
E-mail: junseong@korea.ac.kr

16163028, 0, Downloaded from https://advanced.onlinelibrary.wiley.com/doi/10.1002/adfm.202519859 by Inkyu Park - Korea Advanced Institute Of , Wiley Online Library on [10/12/2025]. See the Terms and Conditions (https://onlinelibrary.wiley.com/terms-and-conditions) on Wiley Online Library for rules of use; OA articles are governed by the applicable Creative Commons License

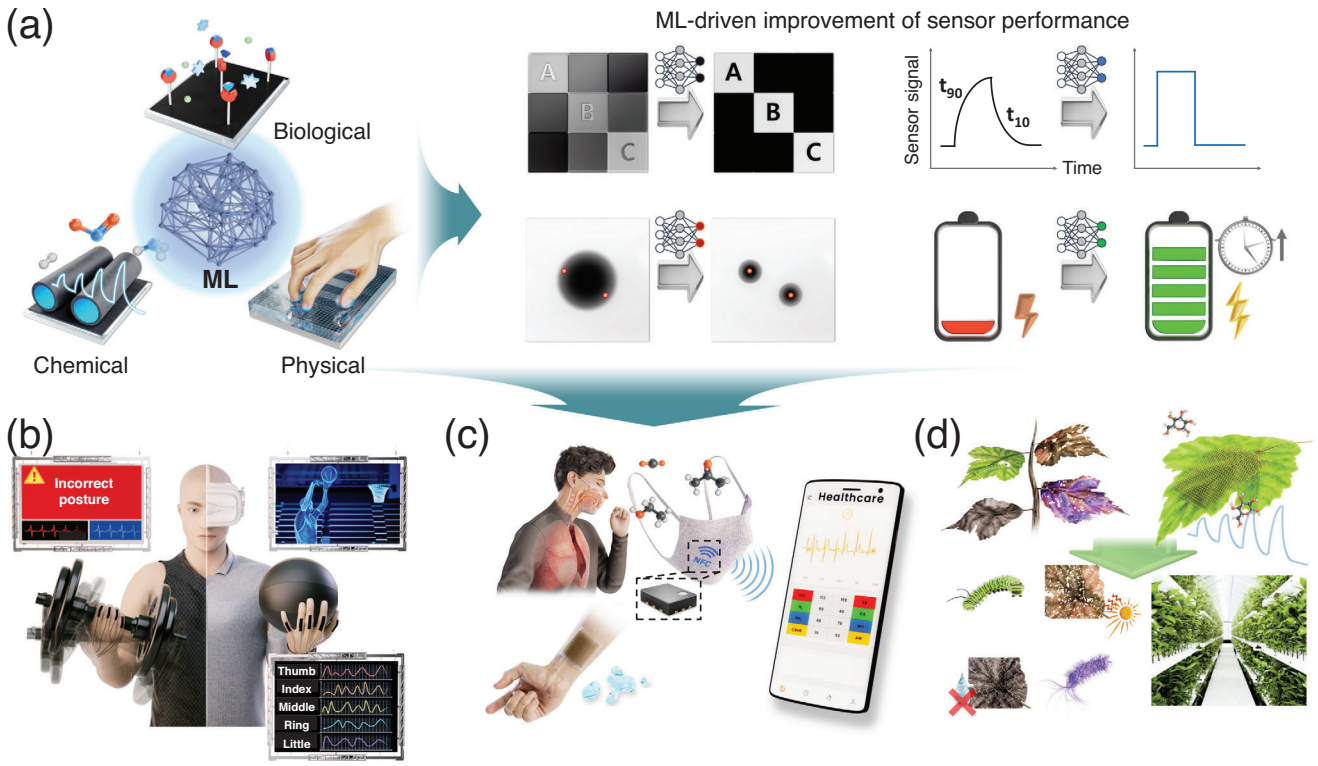

Figure 1. Overview of ML-assisted sensor systems that enhance key performance metrics and enable next-generation applications. a) ML-based optimization improves sensor selectivity, response time, spatial resolution, and energy efficiency. b) Wearable sensors for real-time motion monitoring and AR/VR interfaces through localized, accurate sensing. c) Health monitoring via gas and biomarker detection for early disease diagnosis. d) Smart farming applications using gas sensing from plants to identify specific types of stress and support timely adaptive responses.

selectivity and are sometimes limited by slower response times compared to physical sensors (e.g., strain, pressure, tactile, and shear stress sensing),[48–50] elastomer-based physical sensors suffer from low spatial resolution due to fabrication challenges,[51] and plasmonic-based optical/biological sensors require long analysis times due to manual peak detection.[52] These constraints present critical obstacles to the practical deployment of next-generation sensors.

To overcome these challenges, advancing software-driven approaches alongside hardware improvements is essential. Recent trends indicate that machine learning (ML) is emerging as a powerful tool for sensor signal processing, effectively addressing the inherent limitations of conventional sensors.[53] While ML techniques were initially explored primarily in vision-based sensors, their applications have rapidly expanded to physical and chemical sensors in recent years.[54] Traditional ML methods such as support vector machines (SVMs), k-nearest neighbors (KNN), and principal component analysis (PCA) perform well for simple classification or dimensionality reduction tasks. However, the recent adoption of deep neural networks (DNNs), a subset of ML, has marked a turning point, as DNNs can learn hierarchical features and nonlinear relationships directly from raw data without manual feature engineering.[55] This fundamental difference enables significantly enhanced performance in complex sensing scenarios.

For example, in chemical sensing, ML, particularly DNN, has been employed to enhance selectivity and response time by accurately identifying analytes and predicting their concentrations.[56–58] In physical sensors, ML models have contributed to enhancing spatial resolution, while in spectroscopic sensing, DNN have significantly reduced analysis times by automatically classifying major peaks in Surface-Enhanced Raman Scattering (SERS) spectroscopy, enabling real-time detection.[59] These advancements illustrate that ML not only addresses fundamental limitations of traditional sensors but also broadens their application scope.

Ongoing research continues to explore the integration of ML with advanced sensors and the development of ML-optimized sensor hardware. However, most existing reviews have primarily focused on system-level device-to-device communication or vision sensors for automotive applications.[60,61] There remains a lack of comprehensive reviews that systematically examine ML algorithms aimed at enhancing key performance metrics, particularly for widely used physical and chemical sensors.

This review aims to bridge this gap by providing a structured analysis of ML-driven advancements in next-generation multimodal sensors, as shown in **Figure 1**. In Section 2, a brief overview of the ML algorithms commonly used in sensor systems is provided. Section 3 explores how ML-based signal processing improves key sensor attributes, including selectivity, response time, spatial resolution, stability (drift), power consumption, and analysis process. Each subsection categorizes ML techniques based on their targeted performance improvements and highlights promising strategies for overcoming remaining

© 2025 The Author(s). Advanced Functional Materials published by Wiley-VCH GmbH

16163028, 0, Downloaded from https://advanced.onlinelibrary.wiley.com/doi/10.1002/adfm.202519859 by Inkyu Park - Korea Advanced Institute Of , Wiley Online Library on [10/12/2025]. See the Terms and Conditions (https://onlinelibrary.wiley.com/terms-and-conditions) on Wiley Online Library for rules of use; OA articles are governed by the applicable Creative Commons License

Table 1. Summary of representative ML techniques used to enhance sensor performance across key indices, including selectivity, response time, spatial resolution, and power efficiency. For each index, commonly used ML algorithms, sensor types, electrical output signal characteristics, and typical application areas are presented.

Sensor performance indices	ML algorithms	Types of sensors	Applications	Refs.
Selectivity	SVM, LDA, RF, PCA, KNN, CNN, RNN, Transformer	Chemiresistive, electrochemical, NDIR, PID, cataluminescence, colorimetric, SPR-based, fluorescence and FET-based sensors	Discrimination of bio/organic molecules, cells, and illicit drugs. Food and water safety monitoring and disease diagnosis.	[56,69,71,77,138,142]
Response time	CNN, RNN	Chemical and bio sensor	Detection of biochemical substances.	[70,78]
Spatial resolution	CNN, SVM, ANN, KNN	EIT	Letter recognition.	[101]
Stability (drift)	CNN, LSTM, RNN,	Chemical sensor and fiber optic gyroscope	Correction of drift phenomenon in sensor signal.	[102]
Power consumption	SNN	Image and gas sensors	Mobilization of sensor requiring data compression and communication with low power consumption.	[124]
Automated analysis	ANN, Transformer	SERS	SERS spectral data analysis.	[59,68,125]

challenges, as shown in Figure 1a. Section 4 discusses the real-world applications of ML-enhanced sensors, including human motion monitoring, early-stage disease diagnosis, and plant stress detection for smart farming, as illustrated in Figure 1b–d. To support practical implementation, **Tables 1** and 2 provide an organized overview of ML applications in next-generation sensing platforms. Table 1 classifies representative ML approaches according to sensor performance indices, commonly used sensor types, output characteristics, and application domains. Table 2 presents a deeper analysis of specific sensor applications, highlighting detailed ML structures, preprocessing strategies, hyperparameter tuning, and resulting performance metrics. Section 5 presents a critical discussion on current limitations of ML-integrated sensors and explores future research directions for further advancements. Finally, Section 6 provides concluding remarks on the role of ML in revolutionizing sensor technologies.

2. Brief Overview of ML Algorithms in Sensor Applications

With the increasing integration of ML into sensor systems, the terms artificial intelligence (AI), ML, and DNN are often used interchangeably. Before delving into the core of this review, we clarify these terms. AI broadly refers to computer systems that mimic human decision-making and reasoning, including rule-based systems where actions are triggered by predefined conditions (e.g., turning on the air conditioner if the temperature exceeds a certain threshold). ML is a subset of AI that learns decision rules directly from data, without explicit programming of those decision rules. DNN is a further subfield of ML that uses artificial neural networks (ANN) with typically more than three hidden layers.[62,63]

In sensor data analysis, ML may operate directly on sensor outputs, apply preprocessing for feature extraction, or leverage feature learning to automatically capture informative patterns from raw data. Model selection is guided by the characteristics of the data and the intended task, such as regression, classification, or clustering. The complexity of the model is adjusted to fit the size and quality of the dataset.

When working with limited datasets, overfitting becomes a critical concern. To address this issue, several strategies are commonly applied. Cross-validation partitions the dataset into multiple training and validation folds, and the averaged results across folds yield a more reliable measure of generalization. Data augmentation is used when large datasets are hard to obtain. It enlarges the dataset with controlled variations (e.g., rotation, noise, scaling), helping the model learn robust patterns without extra raw data. Early stopping mitigates overfitting by monitoring validation performance and halting training once it ceases to improve. The model parameters corresponding to the best validation score are then retained.

These procedures are closely linked to the intrinsic properties of sensor data. Understanding this relationship provides a solid foundation for designing robust ML-enhanced sensor applications. This section focuses exclusively on ML- and DNN-based algorithms applied to sensor applications, with a particular emphasis on physical and chemical sensors. It also provides general guidelines on which models are suitable depending on the data characteristics. A timeline of how ML has been applied in sensor-related fields is clearly summarized in **Figure 2** for intuitive understanding.

From a methodological perspective, ML approaches can be broadly categorized into three types: supervised, unsupervised, and reinforcement learning. Supervised learning, which utilizes labeled data, is widely applied to sensor tasks such as selective classification of different analytes and regression-based prediction of their concentrations. Unsupervised learning extracts meaningful patterns from unlabeled data and is mainly used for preprocessing or anomaly detection (e.g., PCA, clustering). Reinforcement learning relies on reward-based feedback to guide decisions, but it is less common in the types of sensors covered here.

In the early stages of ML in sensing (1990s to early 2010s), simple models such as PCA, SVM, KNN, and decision tree models were widely used. PCA, as an unsupervised method, was employed for dimensionality reduction and visualization.[64,65] SVM, KNN, and decision trees are supervised learning methods and were used for classification or regression tasks.[66–68] These models are easy to implement and work well with simple datasets;

© 2025 The Author(s). Advanced Functional Materials published by Wiley-VCH GmbH

Table 2. Detailed case studies of ML-enhanced sensor applications. Each example presents the specific sensor type, ML model structure (including preprocessing pipeline and hyperparameters), and reported performance outcomes, providing practical insight into real-world implementation strategies.

Applications	Sensors	ML algorithms	Model structure	Results	Refs.
Non-invasive disease diagnosis via exhaled breath analysis	MDFG gas sensor array	SVM, CNN	Preprocessing: feature selection (Boruta algorithm) and noise correction (filtfilt function). SVM: Monte Carlo cross-validation, 1D CNN: kernel size: 7, stride: 1, batch size:64, epochs: 20, Lr: 4×10^{-4}, dropout: 0.09, ReLU	Classification accuracy: 98.7% (SVM), 100% (1D CNN)	[69]
Colorimetric sensor-based pathogen monitoring for food safety	Agar gel-based colorimetric sensor arrays	PCA, LDA, CNN	CNN: five hidden layers, Lr: 2×10^{-2}	Four pathogen classification: Accuracy > 80%, precision > 0.86, recall > 0.83 and F1 score > 0.91	[76]
Discriminate of purines	Surface plasmon resonance imaging sensor with GO/rGO	RF, ResNet-based CNN	ResNet-18 and ResNeXt-50 (32 × 4d), 3-channel image input (RGB transformation), 4 output classes, dropout, ReLU, Lr: 8.8×10^{-6}, epochs: 20	Classification accuracy: RF model < 50%, CNN model – validation accuracy: 85%, test accuracy: 78%	[77]
Detecting industrial hazardous gas	Chemiresistive gas sensor	CNN	2D CNN layer with 4 × 5 kernel. 2 FC layer with 10–20 nodes.	Classification accuracy: 97.95% Concentration error: 14%. Response time < 10 s.	[70]
Biomaterial detection	Frequency change with bioreceptor	RNN, ANN	2 RNN layer with 128 nodes, 1 FC layer with 128 nodes (for classification) 1 FC layer with 128 nodes (for forecasting)	Concentration classification with F1 score > 0.85 and response time < 30 min	[78]
Handwritten Letters	Piezoresistive film sensor	1D CNN	1D CNN with MaxPooling, Dropout, FC layer. Cross-entropy loss function, Adam optimizer,	Letter recognition >92%	[101]
Discriminating grapes in wine	Chemiresistive gas sensor	SNN	2 SNN layer with 2 nodes	Processing power consumption < 500 nW	[124]
Bacteria classification in various media	SERS substrate	ANN with Transformer	3 ANN layers with 15–128 nodes	Classification accuracy: 84–96% Without analysis procedure	[125]
Gas discrimination of mono-gas	Multi µLED-based gas sensors	2D CNN	2D CNN: kernel size: 2 × 10, stride: 1, epochs: 1000, Lr: 10^{-4}, Leaky-ReLU, BN, 4 FC layers, Adam optimizer, 2 output nodes: classification and regression, postprocessing (noise filter)	Classification accuracy: 99.3% Regression error: 13.8% (MAE)	[126]
Gas discrimination of mixed-gas	Single µLED-based gas sensor	2D CNN	2D CNN: Avg. pooling, stride: 5, epochs: 130, Leaky-ReLU, BN, 4 FC layers, Adam optimizer, 2 output nodes: classification and regression, postprocessing (noise filter).	Classification accuracy: 98.0% Regression error: ≈34.0% (MAE) for mixed gas	[58]
Sign language recognition	Triboelectric smart glove	1D CNN	Non-segmentation CNN: Four 1D convolutional layers, flatten and dense layers. Segmentation CNN with four Conv. layers, ReLU, flatten and dense layers.	Non-segmentation CNN accuracy of 91–95% Segmentation CNN accuracy of 86.7%	[129]
Gesture recognition	Data glove with MWCNT sensors	CNN–LSTM	CNN–LSTM: CNN block (Depth-wise Conv and Point-wise Conv), LSTM Block, Softmax.	CNN–LSTM achieves > 97% accuracy on 30 gestures	[134]
Object recognition	Triboelectric sensor array	SVM, MLP	Multiclass SVM. MLP: Three hidden layers each with 20 neurons (ReLU) and Softmax.	≈98.6% accuracy in recognizing objects	[135]

(*Continued*)

© 2025 The Author(s). Advanced Functional Materials published by Wiley-VCH GmbH

16163028, 0, Downloaded from https://advanced.onlinelibrary.wiley.com/doi/10.1002/adfm.202519859 by Inkyu Park - Korea Advanced Institute Of , Wiley Online Library on [10/12/2025]. See the Terms and Conditions (https://onlinelibrary.wiley.com/terms-and-conditions) on Wiley Online Library for rules of use; OA articles are governed by the applicable Creative Commons License

Table 2. (Continued)

AR/VR and metaverse	Ring consists of triboelectric and pyroelectric sensors	PCA, SVM	PCA: dimension-reduction, SVM: Radial Basis Function kernel.	≈99.8% on a 14-gesture dataset	[137]
Rapid COVID-19 screening through exhaled breath analysis	E-nose consists of 10 SMO gas sensors	SVM, LDA, MLP, DNN	- Feature Extraction: Extracted maximum, median, standard deviation, and variance from 10 sensors. (40 features per sample) - SVM: Preprocessing (StandardScaler), hyperparameter tuning (grid-search optimization), cost value: 10 - LDA: N.Q. - MLP: Preprocessing (MinMaxScaler), TPOT - DNN: epochs: 500, two dropout layers (0.1), ReLU, Adam optimizer, 10-fold cross-validation	Best Results: DNN. Sensitivity: 95.5%, Specificity: 95.7%, AUC: 95.6%	[139]
Real-time odor prediction and food freshness monitoring	A 10 × 10 metal-oxide–based gas sensor array	CNN	(1) Classification: Input, 10 × 10 heat map based on a sensor's resistance values. 4 CNN layers with pooling layer, ReLU, dropout (0.5), and 2 FC layers. Output, 8D vector passed to LogSoftmax. Epochs: 500. (2) Concentration regression: Input, 10D feature vector extracted via PCA. 5 FC layers	(1) Classification accuracy: 99.04% (2) Regression error (MAE): ≤3% (800 ppb)	[140]

N.C.: not considered; N.Q.: not quantified; SMO: semiconductor metal oxides; GO: graphene oxide; rGO: reduced graphene oxide; SERS: surface-enhanced Raman spectroscopy; E-nose: electronic nose; μLED: micro-light-emitting diode; KNN: k-nearest neighbors; RF: random forest; MLP: multilayer perceptron; TPOT: tree-based pipeline optimization tool; AUC: area under the curve; PCA: principal component analysis; LDA: linear discriminant analysis; SVM: support vector machine; CNN: convolutional neural network; DNN: deep neural network; SNN: spiking neural network; RNN: recurrent neural network; ReLU: rectified linear unit (activation); BN: batch normalization; Lr: learning-rate, FC: fully-connected, Conv: Convolutional MAE: mean absolute error

© 2025 The Author(s). Advanced Functional Materials published by Wiley-VCH GmbH

16163028, 0, Downloaded from https://advanced.onlinelibrary.wiley.com/doi/10.1002/adfm.202519859 by Inkyu Park - Korea Advanced Institute Of , Wiley Online Library on [10/12/2025]. See the Terms and Conditions (https://onlinelibrary.wiley.com/terms-and-conditions) on Wiley Online Library for rules of use; OA articles are governed by the applicable Creative Commons License

16163028, 0, Downloaded from https://advanced.onlinelibrary.wiley.com/doi/10.1002/adfm.202519859 by Inkyu Park - Korea Advanced Institute Of , Wiley Online Library on [10/12/2025]. See the Terms and Conditions (https://onlinelibrary.wiley.com/terms-and-conditions) on Wiley Online Library for rules of use; OA articles are governed by the applicable Creative Commons License

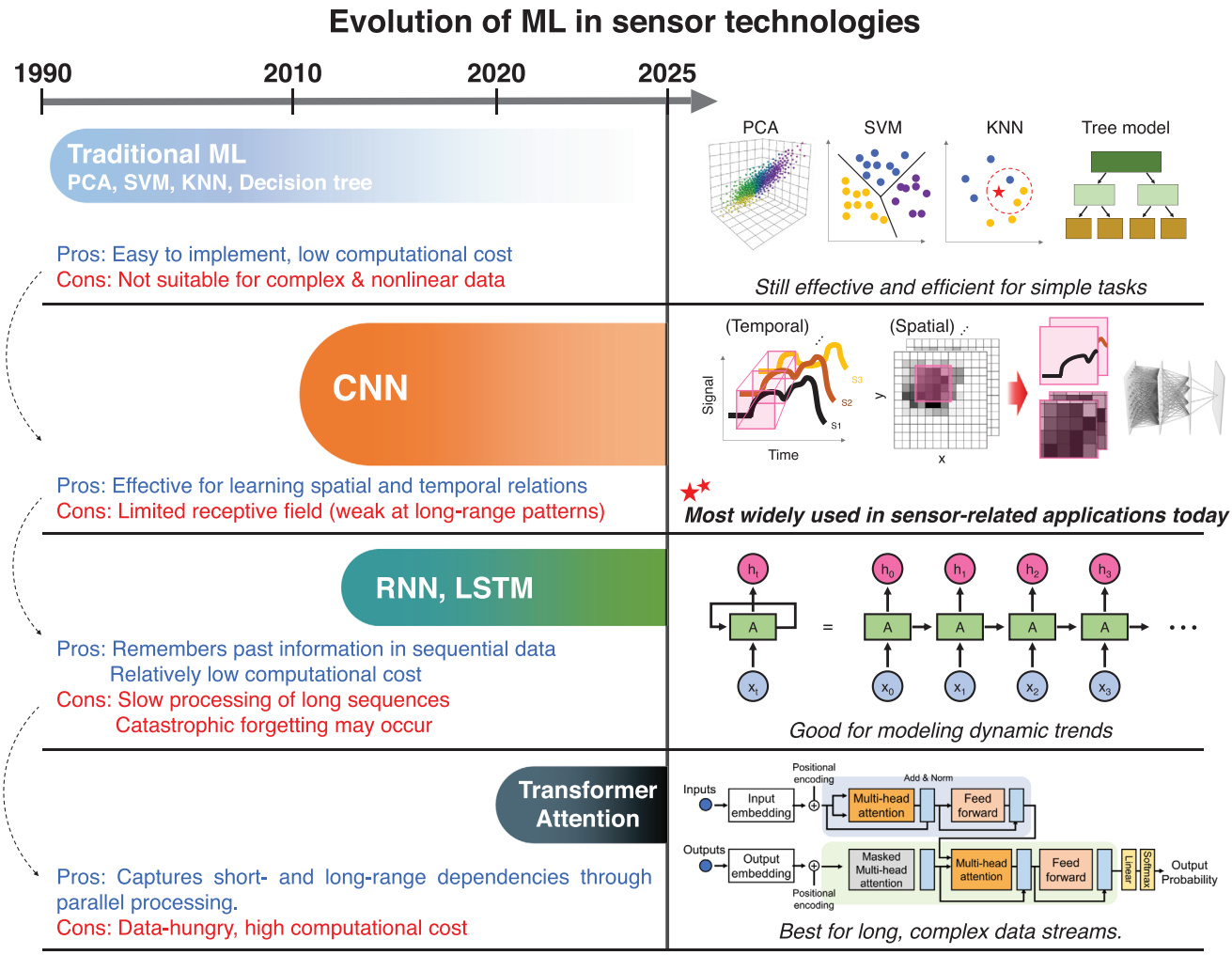

Figure 2. Timeline-style schematic illustrating the progression from traditional ML algorithms (PCA, SVM, KNN, decision tree) to CNN, RNN/LSTM, and Transformer-based models. Key advantages and limitations at each stage are highlighted to explain the shift toward more advanced and scalable approaches.

therefore, they are still widely used. However, they require manual feature engineering, where relevant features must be extracted from raw sensor data prior to training. They also struggle with nonlinear sensor behavior, where the output does not scale linearly with the input, and with high-dimensional, time-series data from sensor arrays.

As sensing tasks became more complex, with larger sensor arrays and greater data volume, DNN emerged as a solution to not only model nonlinear responses but also show potential to find spatiotemporal dependencies within the data volume. Since the mid-2010s, convolutional neural networks (CNNs) have become particularly useful, as they preserve local structure in both spatial and temporal domains. Unlike traditional models that flatten inputs, CNNs extract features from raw sensor signals by preserving the local correlations between adjacent data points. This allows CNNs to effectively analyze temporal changes in gas sensors and spatial stress distributions in physical sensors.[69,70]

When sensor data includes long sequences, temporal modeling becomes essential. Recurrent neural networks (RNNs) and their improved variant, long short-term memory (LSTM), are suited for such tasks due to their ability to retain and update past information. These learning models have been used to track dynamic gas concentration changes or interpret temporal tactile patterns. RNNs and LSTMs, which retain temporal information, have a better temporal receptive field compared to CNNs in handling dynamic sensor data.

Since ≈2020, Transformer architectures have drawn attention in the sensing field.[71,72] These models use attention mechanisms to identify and correlate the most relevant parts of the input sequence, learning long-range dependencies for accurate classification/regression. They are particularly well-suited for processing sequential, high-dimensional, and time-dependent sensor data, such as peak-to-peak correlation in spectral data.

However, optimizing parameters such as the number of layers and nodes remains largely empirical, as solid theoretical guidelines are lacking. Models must be sized to match task complexity: undersized models risk underfitting, while oversized models may overfit when training data are limited. To improve generalization, strategies such as cross-validation, dropout, data augmentation, and early stopping with a validation set are

© 2025 The Author(s). Advanced Functional Materials published by Wiley-VCH GmbH

16163028, 0, Downloaded from https://advanced.onlinelibrary.wiley.com/doi/10.1002/adfm.202519859 by Inkyu Park - Korea Advanced Institute Of , Wiley Online Library on [10/12/2025]. See the Terms and Conditions (https://onlinelibrary.wiley.com/terms-and-conditions) on Wiley Online Library for rules of use; OA articles are governed by the applicable Creative Commons License

commonly employed. While unsupervised learning is also actively explored, this review primarily focuses on supervised applications of CNNs, RNNs, and Transformers in sensor applications.

3. Enhancing Sensor Parameters Using ML

As sensor technology advances for IoT, mobile, and wearable applications, improving key performance indices such as selectivity, response time, spatial resolution, power consumption, and analysis time has become crucial. However, hardware-based improvements alone face limitations due to material constraints and fabrication challenges. To address these issues, ML has emerged as a powerful tool for sensor signal processing, enabling software-driven enhancements that optimize sensor performance. This chapter reviews recent ML-driven advancements in sensor technology, categorizing improvements across major performance parameters. Each section examines the limitations of conventional sensors, ML-based enhancements, and case studies demonstrating successful applications. Additionally, hybrid approaches combining multiple ML techniques are discussed to highlight emerging trends. Through this structured analysis, this chapter provides insights into the current state and future potential of ML-integrated sensors.

3.1. Selectivity

Selectivity refers to the ability to distinguish target analytes (e.g., gas, liquid, ion) from other substances or conditions in the measurement environment. This chapter focuses on applying ML in chemical and biosensors, where nonlinear data make ML particularly effective for enhancing selectivity. Selectivity is particularly important when processing complex mixtures or identifying harmful substances amidst benign ones.[73–75] However, relying solely on the magnitude of signals generated by different analytes can lead to overlapping signals depending on their concentrations, posing a significant challenge to address (**Figure 3a**). ANN, particularly those used in supervised learning with true labels and corresponding training data, are widely employed due to their ability to learn complex, nonlinear relationships between inputs and outputs. This capability, enabled by activation functions and multi-layer architectures, makes ANN particularly effective for enhancing selectivity in chemical sensing applications. Moreover, achieving high selectivity often involves using sensor arrays with distinct response patterns, which ML algorithms can analyze to classify analytes and conditions more effectively.

Hwang et al. addressed this by developing a multiplexed DNA-functionalized graphene (MDFG) gas sensor array integrated with ML for non-invasive disease diagnosis via exhaled breath analysis (Figure 3b).[69] Human breath comprises complex gases under high humidity, demanding robust sensors. Graphene was chosen for its room-temperature operation, while single-stranded DNA (ssDNA) was used to functionalize its surface, enhancing sensitivity and selectivity through specific gas interactions. The MDFG array included seven channels: three functionalized with single ssDNA sequences (A6, T6, G6), three with combinations (A6T6, A6G6, T6G6), and one pristine graphene channel serving as a control. This configuration enabled the detection of gases such as NH_3, NO, NO_2, and H_2S, as well as their mixtures at varying ratios. To minimize noise, the Boruta algorithm—a random forest (RF)-based wrapper method that removes irrelevant variables by comparing their importance to that of shadow features, which are randomized copies of the original variables—was used for feature selection, followed by classification using SVM, which achieved over 98% recognition rates under low and high humidity. A 1D CNN further improved performance, achieving 100% accuracy across all tested conditions, including mixed gas compositions. However, their classification framework relied on supervised learning, treating each gas mixture ratio as a distinct label based on predefined categories. This approach limits the model's ability to generalize to untrained gas mixture ratios, as it lacks regression capabilities for estimating concentrations. In Chapter 3.5, advanced dual-task ML models that combine gas type classification with regression-based concentration predictions will be discussed to address this limitation.

Colorimetric sensors, which use dyes to indicate analytes through visible color changes, are commonly applied in food safety but face challenges such as interference from volatile organic compounds (VOCs) and limited selectivity. Zhang et al. enhanced selectivity by integrating ML with an agar-based colorimetric sensor array (Figure 3c).[76] Their system utilized 16 dyes grouped into amphoteric solvent-changing dyes, pH indicators, metal ion-containing dyes, and pathogen-specific reactive dyes. These dyes were embedded into agar gel microdots, chosen for their stability, high surface area for rapid VOC diffusion, and resistance to humidity-induced distortions. Analyte-induced color changes were captured via a smartphone camera and digitized into 48 RGB chromaticity values (16 dye spots × 3 RGB). These color patterns were then classified using PCA and linear discriminant analysis (LDA). Additionally, ANN model was employed, achieving a precision of 0.86, a recall of 0.83, and an F1-score of 0.91 when distinguishing four pathogens. Here, precision is defined as the number of true positive predictions divided by the total number of positive predictions (true positives + false positives), indicating the accuracy of positive predictions. Recall is the number of true positives divided by the total number of actual positives (true positives + false negatives), measuring how well the model detects all actual positive cases. To jointly evaluate the performance of precision and recall, the F1-score, defined as the harmonic mean of the two ($F1 = 2 \times (Precision \times Recall) / (Precision + Recall)$), can be used, where a value closer to 1 indicates better overall performance. The system demonstrated real-world efficacy by testing eggshells inoculated with *Staphylococcus aureus* and *Listeria monocytogenes*, achieving over 80% accuracy despite the presence of interfering compounds. This highlights its potential for real-world applications in food safety monitoring.

Surface plasmon resonance imaging (SPRi) is a label-free sensing technique that measures refractive index changes near sensor surfaces with high spatial resolution. It generates 2D intensity maps of time-dependent changes in reflected light, serving as ML input for analyte classification. However, detecting small molecules like purines is challenging due to their minimal refractive index changes. Jobst et al. addressed this using a semi-selective receptor array composed of graphene oxide (GO) and reduced graphene oxide (rGO) to classify purines, including adenine, caffeine, oxipurinol, and uric acid (Figure 3d).[77]

© 2025 The Author(s). Advanced Functional Materials published by Wiley-VCH GmbH

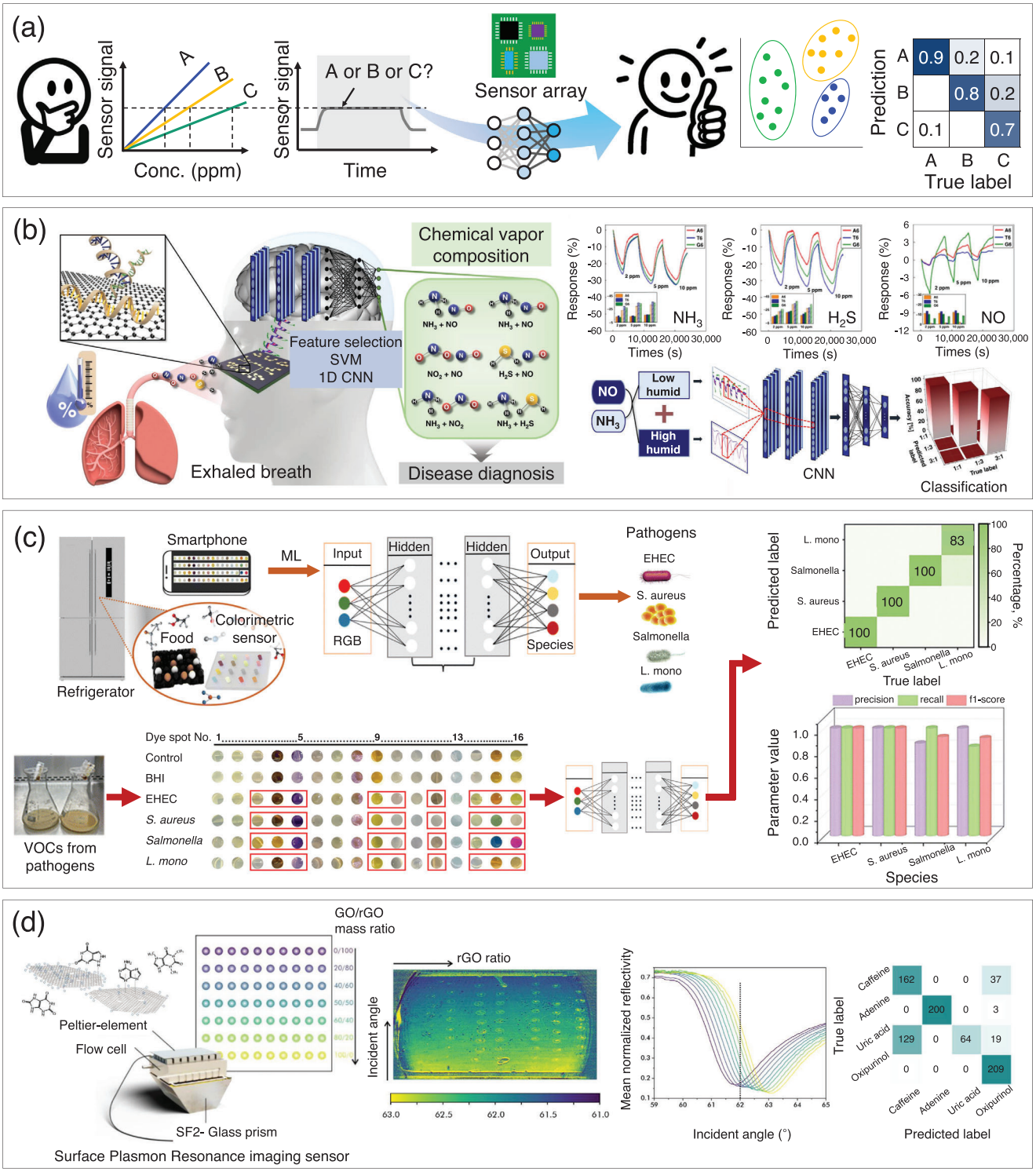

Figure 3. Improving sensor selectivity with ML. a) Challenges in sensor selectivity due to overlapping signals, addressed by combining ML with sensor arrays. b) MDFG gas sensor array using ssDNA functionalization detects individual gases and mixtures accurately under varying humidity conditions, reproduced under the terms of the CC-BY-4.0 license,[69] Copyright 2023, The Authors. c) Agar-based colorimetric sensor array with selective dyes for food safety applications, where ML analyzes color patterns to classify pathogens, reproduced with permission,[76] Copyright 2023, The Royal Society of Chemistry. d) SPRi with GO/rGO receptor arrays tailored for purine classification. CNN processed intensity maps to detect similar molecules with high accuracy, reproduced with permission,[77] Copyright 2023, American Chemical Society.

© 2025 The Author(s). Advanced Functional Materials published by Wiley-VCH GmbH

16163028, 0, Downloaded from https://advanced.onlinelibrary.wiley.com/doi/10.1002/adfm.202519859 by Inkyu Park - Korea Advanced Institute Of , Wiley Online Library on [10/12/2025]. See the Terms and Conditions (https://onlinelibrary.wiley.com/terms-and-conditions) on Wiley Online Library for rules of use; OA articles are governed by the applicable Creative Commons License

GO and rGO facilitated weak interactions such as π-stacking and hydrogen bonding. By fine-tuning GO/rGO ratios, unique response patterns were created for each purine. The RF model achieved an accuracy of below 50%, whereas the CNN achieved a validation accuracy of 85% and a test accuracy of 78%. The results confirmed that SPRi combined with ML enables the detection and classification of structurally similar small molecules by generating specific responses through high-affinity receptors. This approach demonstrates potential applications in environmental monitoring, biomedical diagnostics, and industrial safety.

These examples demonstrate the effectiveness of integrating ML with sensor technologies to significantly enhance selectivity. In particular, they highlight the ability to selectively identify target substances even in complex environments where overlapping signals or similar responses occur. Notably, increasing the number of sensors can broaden the range of distinguishable analytes and improve accuracy, but excessive use may cause higher power consumption, larger device size, and overfitting, reducing generalizability. Recent studies also show that novel driving methods, such as pulsed operation, can retain information while using fewer sensors, thereby improving efficiency.[41,58] Furthermore, while this chapter primarily focused on chemical sensors, ongoing research continues to explore the application of ML to sensor systems, paving the way for multi-modal selective sensing capable of handling mixed stimuli or inputs in diverse scenarios. Improvements in selectivity has already enabled real-world applications in areas such as healthcare, food monitoring, and smart farming, as discussed in greater detail in Chapter 4.2.

3.2. Response Time

The definition of response time varies slightly across fields, but in the context of sensors, it is generally quantified as the T_{90} time. This represents the duration required for a sensor's response to reach 90% of its saturation level after applying a step function input. The T_{10} time is referred to as the recovery time, defined as the time required for the response to decrease to 10% when the external stimulus is removed. The definition of these terms differs slightly from other fields, such as control engineering, where rising and falling times are typically defined as transitions between 10% and 90%, or vice versa. Slow response times in sensors hinder the immediate collection of accurate data. This is particularly problematic for sensors designed for multimodal data collection, as low temporal resolution increases the risk of interference between different types of information. In the left graph of **Figure** 4a, the gray curve represents the response of a sensor with a large response time. Based on the current data, it is challenging to predict where the future response (orange line) will be saturated. However, by training an ML model on the time-series data of the sensor's transient response, it becomes possible to quickly predict the saturation point of the sensor within a short time, as shown by the blue curve in the right graph of Figure 4a. Speed compensation can sometimes be achieved using regression techniques based on specific equations, but such methods are limited when the sensor's response cannot be easily modeled. In contrast, applying ML to the sensor's time-series data enables the rapid extraction of desired information, even from sensors with unknown or complex characteristics that are theoretically difficult to model.[78–84]

Specifically, chemical sensors used in electronic nose (e-nose) systems and biosensors for analyzing biological substances often suffer from slow response times. In such scenarios, an ANN with a few layers and tens to hundreds of nodes can be used to improve response speeds. CNNs are highly suitable for analyzing patterned data, time-series data, or 2D images. RNNs are also advantageous for analyzing long time-series data. Therefore, understanding how sensor's response characteristics are reflected in the data and accordingly designing proper neural network models with a sufficient number of layers and nodes is crucial.

For example, Orbe et al. developed a low-power multi-gas sensor array to accurately detect flammable and toxic gases, employing a CNN algorithm to quickly classify and measure the concentration of each gas, as described in Figure 4b.[70] Specifically, four types of sensors were integrated into a MEMS platform consisting of bridge-type microheaters. The array was designed using three different mechanisms, chemiresistive, catalytic combustion, and calorimetric sensing, with nanostructured materials (ZnO, CuO, and Pt black) integrated onto the microheater sensors, as shown in Figure 4b-i. Although the response and recovery times for the four gas sensors were not explicitly stated, the response time of the metal oxide gas sensors was estimated to be several 100 s (Figure 4b-ii). The transient responses of the four sensors over 5 s were fed into the CNN for real-time classification and regression of five different gases (H_2, NO_2, ethanol, CO, and NH_3) (Figure 4b-iii). As a result, it was possible to rapidly predict the gas concentration within 10 s from the onset of the sensor response, even before signal saturation occurred. In this case, the concentration prediction error was 14% in mean absolute error (MAE) (Figure 4b-iv).

In Figure 4c, Zhang et al. improved the accuracy and response speed of a biosensor for detecting microRNA by classifying its response using an RNN and an ANN.[78,85] Specifically, a cantilever-type biosensor functionalized with DNA that changes its resonant frequency was developed to detect let-7a miRNA at concentrations ranging from 1 nM to 100 fM, as shown in Figure 4c-i. The time required for the response of the sensor to reach saturation varied from 40 to 80 min, depending on the experimental conditions (Figure 4c-ii). This study enabled the prediction of concentrations using only the response of the initial 10 min before saturation by using a combination of RNN and ANN with a time window of 20 points from the sensor response. The 20-point time-series data were sequentially processed by the RNN. Finally, the output of the final hidden layer was transferred to a fully-connected layer to predict the concentration and type of target RNA (Figure 4c-iii). The classifier developed in this study enabled the quantification of analyte concentration and incorrect results with an average prediction accuracy, precision, and recall of 98.5%, significantly reducing the data acquisition time to 5–20 min (Figure 4c-iv).

Martvall et al. developed a self-attention-based ensemble model, termed the Long Short-Term Transformer Ensemble Model for Accelerated Sensing (LEMAS), to improve the response time of plasmonic hydrogen sensors that leverage changes in the localized surface plasmon resonance of palladium-based nanostructures.[79] Conventional plasmonic hydrogen sensors typically rely on equilibrium peak-centroid

© 2025 The Author(s). Advanced Functional Materials published by Wiley-VCH GmbH

16163028, 0, Downloaded from https://advanced.onlinelibrary.wiley.com/doi/10.1002/adfm.202519859 by Inkyu Park - Korea Advanced Institute Of , Wiley Online Library on [10/12/2025]. See the Terms and Conditions (https://onlinelibrary.wiley.com/terms-and-conditions) on Wiley Online Library for rules of use; OA articles are governed by the applicable Creative Commons License

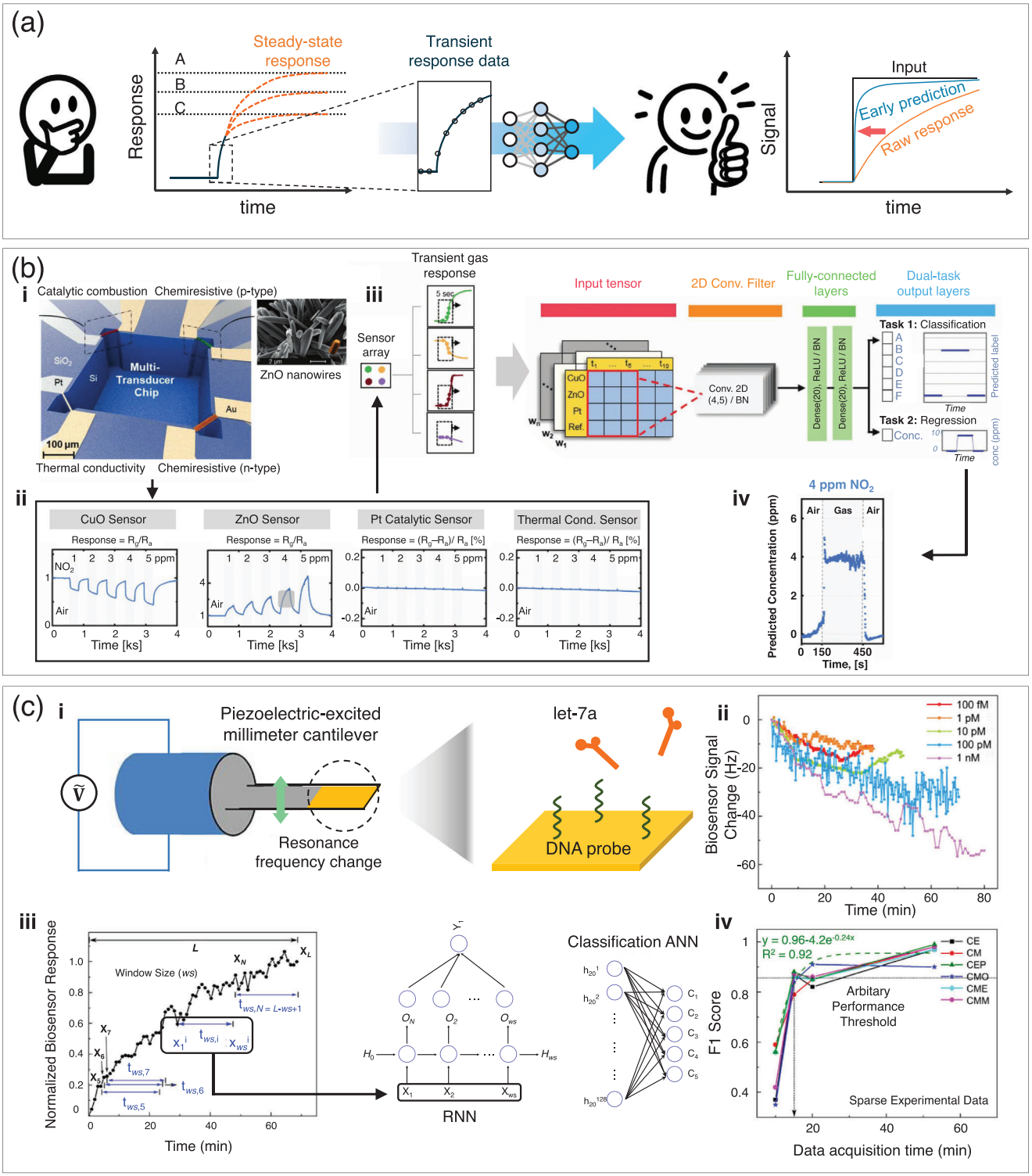

Figure 4. Improving the response time of sensors with ML. a) Challenges in signal identification due to slow sensor response, addressed by combining ML with time-series output data of sensors. b) The CNN algorithm was applied to improve the speed of CuO and ZnO gas sensors to detect 4 ppm NO_2, utilizing the transient response of the sensor output, reproduced with permission,[70] Copyright 2023, Wiley-VCH GmbH. c) RNN and ANN were applied to rapidly extract information from the delayed response of an mRNA sensor detecting let-7a, reproduced with permission,[78] Copyright 2023, Elsevier B.V. All rights reserved.

© 2025 The Author(s). Advanced Functional Materials published by Wiley-VCH GmbH

16163028, 0, Downloaded from https://advanced.onlinelibrary.wiley.com/doi/10.1002/adfm.202519859 by Inkyu Park - Korea Advanced Institute Of , Wiley Online Library on [10/12/2025]. See the Terms and Conditions (https://onlinelibrary.wiley.com/terms-and-conditions) on Wiley Online Library for rules of use; OA articles are governed by the applicable Creative Commons License

16163028, 0, Downloaded from https://advanced.onlinelibrary.wiley.com/doi/10.1002/adfm.202519859 by Inkyu Park - Korea Advanced Institute Of , Wiley Online Library on [10/12/2025]. See the Terms and Conditions (https://onlinelibrary.wiley.com/terms-and-conditions) on Wiley Online Library for rules of use; OA articles are governed by the applicable Creative Commons License

analysis, which limits both their response speed and sensitivity. In this study, the spectral data from the sensor were divided into long-term and short-term sequences, each processed through the LEMAS. The long-term self-attention branch captures global spectral trends, while the short-term branch focuses on recent fluctuations. LEMAS comprises an ensemble of 10 independently trained long short-term Transformer models, whose outputs are averaged to predict the hydrogen concentration. The model's sensing performance was evaluated under leakage scenarios across various hydrogen concentrations. Notably, for H_2 concentrations below 0.1 vol.%, LEMAS achieved a response time, T_{90} of 1.6–3.6 s, representing a 20—40-fold improvement compared to the 50–85 s of conventional single-centroid analysis.

As in the previous cases, ML can be effectively employed to significantly enhance the sensor response time. This is primarily accomplished by utilizing the sensor output as time-series data in CNN or RNN, either to optimize regression algorithms or to classify the magnitude of the response. However, during the supervised learning process, training is typically limited to discrete label values due to the constraints imposed by experimental conditions. Consequently, when the algorithm is applied to input data obtained under conditions not included in the training set, it becomes necessary to demonstrate whether accurate interpolation or extrapolation is feasible for target values which is absent from the training data. Future research is therefore expected to focus on developing algorithms capable of consistently mapping sensor output to a continuous output domain, thereby improving generalizability and robustness across a broader range of sensing conditions.

3.3. Spatial Resolution

Resolution, defined as the smallest detectable change in a measured parameter, is a fundamental performance metric that determines a sensor's ability to precisely distinguish between closely spaced values. Resolution contributes to the overall measurement fidelity by enabling finer discrimination of signal changes. Therefore, it is an essential parameter when evaluating the performance of sensors in applications that require high granularity. Spatial resolution is particularly important in tactile, thermal, and vision sensors. However, since thermal and vision sensors have already been the focus of numerous studies, this work will primarily concentrate on tactile sensors.[86–93] Consequently, we examine tactile-based sensors and their advancements in spatial resolution through the integration of ML techniques, addressing challenges specific to wearable technologies.

For tactile sensors, spatial resolution takes on a unique importance as it determines the sensor's ability to localize contact points and differentiate force variations across its surface. This capability is essential for advanced applications such as robotics, prosthetics, and wearable technologies, where precise touch and force mapping are required. However, achieving high spatial resolution in tactile sensors presents unique challenges, including fabrication complexity, material constraints, and signal inaccuracies caused by nonlinearity and noise. To overcome these challenges, researchers are increasingly leveraging ML, which has proven to be a transformative approach for enhancing spatial resolution (**Figure 5a**).[94–96] In tactile sensors, ML algorithms are pivotal in interpreting complex datasets to extract high-resolution information, addressing the limitations of traditional hardware upgrades. By leveraging ML, it becomes possible to enhance spatial resolution and accuracy without increasing sensor density or complexity. As tactile sensors generate serial data streams, simpler models such as 1D-CNNs and RNNs are often used. Compared to more complex architectures, these networks are easier to implement and train while still excelling at capturing the temporal and spatial patterns crucial for highly accurate signal classification and reconstruction. This balance of simplicity and performance makes them particularly valuable for applications requiring precise, real-time tactile feedback.

Recent studies also demonstrate that structural and material innovations complement ML in advancing spatial resolution. For example, an octopus-inspired adaptive sensor compressed multidimensional touch data into concise signals for accurate multitouch localization,[97] an alterable robotic skin enabled reconfigurable unit density for tunable resolution,[98] and a location–pressure fusion sensor reached sub-400 µm resolution for precise intention recognition.[99]

Electrical Impedance Tomography (EIT) is an imaging technique that reconstructs internal conductivity distributions based on surface electrical measurements. In the field of tactile sensing, EIT-based sensors have gained prominence for their ability to reduce wiring complexity while enhancing spatial resolution. In Figure 5b, Minakawa et al. introduced a hybrid approach to enhance the spatial resolution of EIT by combining the iterative Gauss–Newton algorithm with a 1D-CNN.[94] The Gauss–Newton algorithm, a classical approach for solving nonlinear least squares problems, ensures stable mathematical convergence but suffers from reduced accuracy when resolving small-scale features. By integrating it with a 1D 1D-CNN, the hybrid method improves spatial resolution significantly. Quantitatively, this integration reduces normalized size error (NSE) by more than 27% and normalized positional error (NPE) by ≈29% compared to the 1D-CNN alone when the object-to-background size ratio is below 8.0×10^{-3}. Compared to the conventional Gauss–Newton method, the hybrid approach reduces size error by over 68% across various object sizes, enabling more precise detection of small anomalies. As shown in Figure 5c, Pesce et al. addressed spatial resolution and scalability issues in pressure sensors using electrical resistance tomography (ERT) with a foam mat sensor (FMS).[100] By dividing the 60×60 mm^2 sensor surface into a 3×3 grid, they achieved a functional spatial resolution of 20 $\times$ 20 mm^2 per zone using only 16 electrodes and an opposing current injection scheme. Unlike conventional ERT approaches that require complex inverse image reconstruction, their ML-based classification approach, using algorithms such as SVM and KNN, enabled direct localization of pressure inputs. The system achieved classification accuracies of 87.5% for single-touch and 83.7% for dual-touch scenarios, demonstrating robust zone-level resolution without the computational overhead of tomographic imaging. While sub-zone resolution was not reported, the ability to discriminate between nine distinct zones in real-time highlights a practical enhancement in resolution and scalability for large-area tactile sensing applications. As presented in Figure 5d, Zhang et al. adopted a biologically inspired approach, simplifying sensor architecture while enhancing resolution.[101] By applying quadratic discriminant analysis, they classified signals from

© 2025 The Author(s). Advanced Functional Materials published by Wiley-VCH GmbH

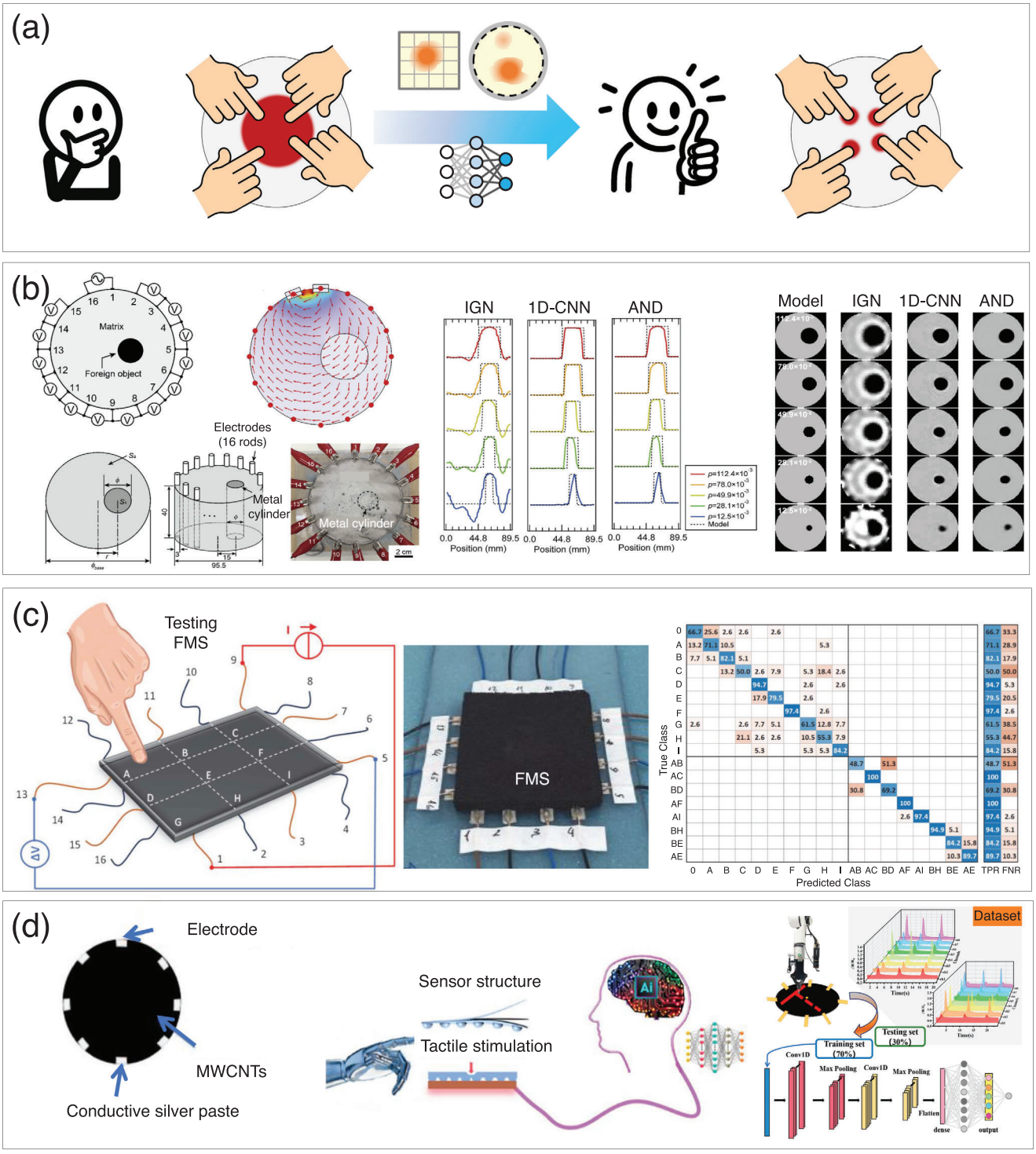

Figure 5. Spatial resolution enhancement through ML. a) Schematic illustration of the spatial resolution enhancement process by ML. b) Resolution improvement of EIT, reproduced under the terms of the CC-BY-4.0 license,[94] Copyright 2024, The Authors. c) Resolution improvement of ERT, reproduced under the terms of the CC-BY-4.0 license,[100] Copyright 2023, The Authors. d) Resolution improvement of flexible large-area tactile sensor, reproduced with permission,[101] Copyright 2024, American Chemical Society.

© 2025 The Author(s). Advanced Functional Materials published by Wiley-VCH GmbH

16163028, 0, Downloaded from https://advanced.onlinelibrary.wiley.com/doi/10.1002/adfm.202519859 by Inkyu Park - Korea Advanced Institute Of , Wiley Online Library on [10/12/2025]. See the Terms and Conditions (https://onlinelibrary.wiley.com/terms-and-conditions) on Wiley Online Library for rules of use; OA articles are governed by the applicable Creative Commons License

only 8 electrodes with 97.5% accuracy across 32 distinct spatial regions. This strategy effectively decouples spatial resolution from the number of physical sensing units, enabling high-resolution perception through data-driven processing.

Although numerous attempts have been made to enhance spatial resolution, ML techniques often require extensive datasets for training, which may not adequately capture real-world conditions. Data acquisition for high-dimensional, multi-contact scenarios remains labor-intensive and susceptible to errors arising from variations in experimental setups. ML-based approaches heavily depend on signal preprocessing and filtering to mitigate noise and artifacts, yet insufficient preprocessing can degrade model performance, particularly in dynamic or noisy environments. Additionally, the fabrication of high-density sensor arrays integrated with ML algorithms presents challenges related to scalability and cost-effectiveness. Advanced materials, such as carbon nanotubes and graphene, demand precise processing techniques, and ensuring uniform performance across large sensor areas is particularly challenging. Despite these obstacles, ML integration has demonstrated remarkable potential in improving spatial resolution and enhancing the performance of tactile sensors. Addressing limitations in hardware complexity, computational efficiency, and data requirements is essential for widespread implementation in applications such as robotics, prosthetics, and wearable technologies. Future efforts should prioritize the development of simplified sensor architectures, the optimization of ML algorithms for real-time processing, and scalable fabrication methods to overcome existing barriers and further advance this field.

3.4. Stability (Drift)

Drift is a phenomenon where a sensor's output fluctuates over time or due to environmental changes, independent of the actual stimulus, and can be attributed to factors such as temperature, humidity, and long-term use. This drift degrades the sensor's precision and repeatability, causing serious problems in applications that demand high reliability. **Figure 6**a intuitively illustrates the problem of a sensor's real-time output deviating from the expected value due to drift, and the solution where an ML model corrects this drift component to stabilize the output. Recently, there have been active efforts to utilize ML techniques to compensate for drift and maintain long-term sensor performance.[102–112]

Badawi et al. proposed a temporal CNN (TCN) architecture based on the Hadamard transform (HT), a generalized discrete Fourier transform in binary matrices, to compensate for sensitivity drift in chemical sensors.[102] In this study, the network was designed with a residual architecture that takes the sensor's time-series signal as input and combines dilation-based causal convolution with a HT block (Figure 6b-i). By applying soft-thresholding in the HT domain, high-frequency noise is removed, enabling smooth drift estimation (Figure 6b-ii). The proposed TCN was validated using both pre-collected chemical sensor data and experimental data from a commercial MQ-137 ammonia sensor, demonstrating its ability to stably estimate and remove drift from actual measurements (Figure 6b-iii). Furthermore, a comparative experiment substituting the HT with the Discrete Cosine Transform (DCT) showed that the Hadamard-based model achieved a 27% lower mean squared error (MSE) overall, indicating its superior drift compensation performance.

In another approach, Mao et al. proposed an ML model based on an LSTM-RNN to compensate for temperature drift in a fiber optic gyroscope (FOG)-based inertial measurement unit (Figure 6c-i).[103] While FOG sensors offer a simple structure and high accuracy, their output is sensitive to temperature variations, which causes drift errors attributable to the Shupe effect (Figure 6c-ii). To address these complex nonlinear characteristics, the researchers used a real-time extraction method for the temperature change rate based on a moving average, which served as an input signal for the processing algorithm (Figure 6c-iii). The performance of the proposed LSTM-RNN model was verified through simulations using field test data from a temperature range of −20–50 °C. The evaluation, based on MAE and root mean squared error (RMSE), showed that the LSTM-RNN model achieved at least 21.9% superior compensation accuracy and stability compared to other models such as an ANN, decision tree, and Online-SVM regression (Figure 6c-iv).

Kwon et al. proposed a novel compensation technique for sensor drift in e-noses, applying the concept of prompt-based learning as an alternative to conventional fine-tuning.[108] This method generates a "calibration feature vector" containing drift information and concatenates it with the original sensor signal as input to a concentration prediction model. This feature vector is generated by a calibration feature encoder based on a masked autoencoder, which learns drift patterns by being trained to reconstruct original data from a randomly masked input. This prompt-based approach allows the model to exhibit robust performance against long-term drift changes with only a single training session, without the need for continuous retraining on new data. Experiments on a publicly available 3-year e-nose dataset, accessible online for research purposes, demonstrated that the proposed method achieved almost 10 times lower RMSE than other comparative models, including a fine-tuned model, thus proving its superior performance.

As demonstrated, applying ML techniques to various sensor platforms has shown significant achievements in improving the long-term reliability and precision of sensors. Models like LSTM-RNN and temporal CNNs effectively compensate for diverse sensor drift phenomena, and it is noteworthy that TCN-based approaches using dilation can be highly effective for time-series data. However, two challenges can be raised regarding this ML approach. First, since sensor drift arises from various sources, including external factors like temperature and humidity, as well as internal factors like sensor contamination and degradation, it remains questionable whether ML can effectively compensate for drift from unknown causes. Second, training these algorithms requires data, and the nature of drift necessitates long-term data collection. Therefore, future research will likely evolve from simple drift compensation toward distinguishing between various causes of drift or even predicting drift before it significantly impacts the performance of sensors.

3.5. Power Consumption and Automated Analysis

To this point, many studies have been introduced that focus on calibrating the output signal of the sensors. Some

© 2025 The Author(s). Advanced Functional Materials published by Wiley-VCH GmbH

16163028, 0, Downloaded from https://advanced.onlinelibrary.wiley.com/doi/10.1002/adfm.202519859 by Inkyu Park - Korea Advanced Institute Of , Wiley Online Library on [10/12/2025]. See the Terms and Conditions (https://onlinelibrary.wiley.com/terms-and-conditions) on Wiley Online Library for rules of use; OA articles are governed by the applicable Creative Commons License

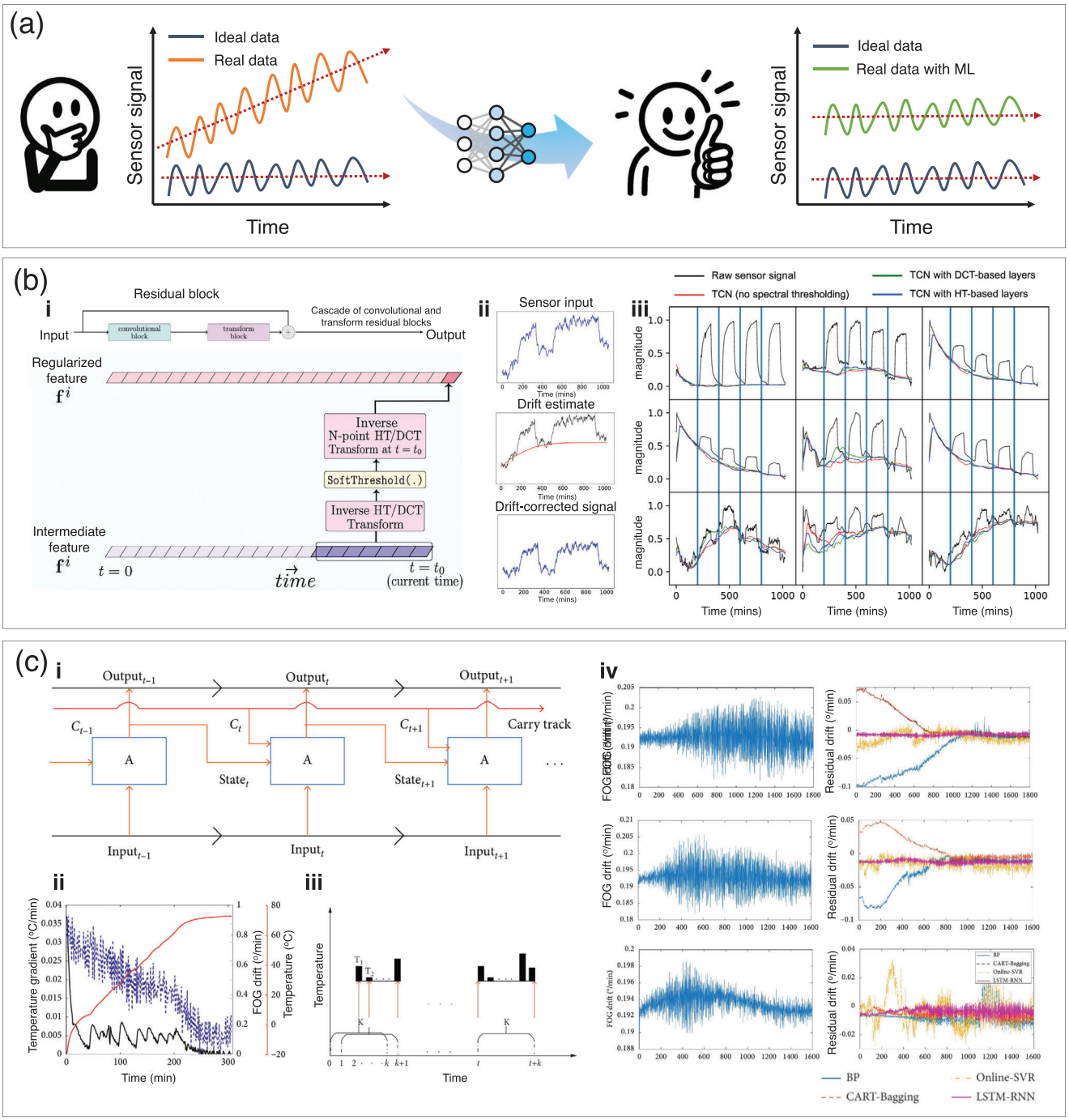

Figure 6. ML-Based Approaches for Sensor Drift Compensation. a) Schematic illustration of stability enhancement process by ML. b) ML-based baseline estimation for signal drift in a chemical sensor based on TCN and HT, reproduced with permission,[102] Copyright 2021, IEEE. c) Drift of the FOG sensor with temperature change compensated by the LSTM-RNN, reproduced under the terms of the CC-BY-4.0 license,[103] Copyright 2021, The Authors. Mathematical Problems in Engineering, published by Wiley-VCH GmbH.

studies have also been conducted to improve other sensor performances, such as accuracy,[113,114] hysteresis,[115–117] and signal-to-noise ratio.[118–120] However, in addition to sensor signal compensation, indirect factors also could be significant issues, such as size, cost, power efficiency, and data analysis method. This chapter aims to present ML-based case studies that address two critical indirect factors: reducing power consumption and automating data analysis. The issue of power consumption is particularly critical in environments where sensors operate on batteries or where a continuous power supply is challenging. Traditional Von Neumann computing architectures are designed to read data from sensors and process it through central

© 2025 The Author(s). Advanced Functional Materials published by Wiley-VCH GmbH

16163028, 0, Downloaded from https://advanced.onlinelibrary.wiley.com/doi/10.1002/adfm.202519859 by Inkyu Park - Korea Advanced Institute Of , Wiley Online Library on [10/12/2025]. See the Terms and Conditions (https://onlinelibrary.wiley.com/terms-and-conditions) on Wiley Online Library for rules of use; OA articles are governed by the applicable Creative Commons License

processing units (CPUs) or analog-to-digital converters (ADCs), which consume significant energy. In contrast, neural network architectures, which mimic the biological nervous system for information processing, can thus be free from the constraints of von Neumann structures. In particular, to circumvent the excessive power and computational costs inherent in Von Neumann architectures, neuromorphic in-sensor computing devices that integrate memory and processing capabilities directly into the sensor have been actively investigated.[121–123]

Figure 7a illustrates the study by Han et al., which demonstrates the development of a neuromorphic e-nose by combining a semiconductor metal oxide (SMO) gas sensor with a single transistor neuron (1T-neuron).[124] As shown in Figure 7a-i, the system utilizes the SMO gas sensor as an olfactory receptor and processes the detected signals into spike forms through the transistor, eliminating the need for additional transducers or CPUs for signal processing. SnO_2 and WO_3 sensors detect resistance changes in response to NH_3 and other gases, which are converted into spike signals via the transistor (Figure 7a-ii,iii). Figure 7a-iv demonstrates how the spiking neural network (SNN) processes these signals to classify gases, such as NH_3, CO, acetone, and NO_2. Figure 7a-v includes a confusion matrix that visually represents the SNN's high classification performance, achieving an accuracy of 98.25% in gas detection. By implementing neural network computations directly in hardware, this approach successfully performed tasks like distinguishing between Shiraz and Merlot wines while reducing power consumption to as low as 350 nW. This research highlights the potential of neuromorphic computing to reduce power consumption and hardware costs in signal processing, while significantly enhancing the energy efficiency of IoT applications.

Reducing analysis time for processing sensor data is a critical factor in real-time applications utilizing sensors. Recently, SERS has gained attention as an effective method for the rapid detection of microorganisms, such as bacteria. However, several challenges must be addressed to miniaturize and mobilize SERS analysis. One of the most significant issues is the processing of SERS spectral data. In SERS measurements, bacterial signals often overlap with solvent signals or coincide with spectral peaks from cell wall proteins, making clear differentiation difficult. Traditionally, statistical methods such as PCA have been employed to address this issue, but these approaches are labor-intensive and difficult to automate. The time required for data analysis can be significantly reduced by employing ML techniques to directly analyze the spectral signals.[59,68,125]

In Figure 7b, Rho et al. demonstrate the development of a novel DNN model, dual-branch wide-kernel network (DualWKNet), applied to the analysis of SERS spectra.[125] Using SERS sensors, spectral data for *E. coli* and *S. epidermidis* were collected in various environments, including water, artificial urine, milk, and nutrient broth (Figure 7b-i,ii). As shown in the figure, the peaks generated by individual bacteria are difficult to distinguish due to interference from the surrounding media, requiring additional processing. This study effectively addressed this challenge by leveraging an ML algorithm that combines residual blocks and self-attention mechanisms, allowing the model to learn critical features from Raman spectra efficiently and achieve high classification performance (up to 98% accuracy) even with limited training data (Figure 7b-iii,iv). Notably, the proposed DualWKNet was able to accurately separate bacterial signals from overlapping media signals without relying on statistical methods like PCA, significantly reducing the time and effort for data analysis. Furthermore, this approach eliminated the need for sample preprocessing, enhancing its practicality across various application environments.

Beyond merely calibrating sensor outputs, the integration of ML with sensor systems offers the potential to significantly reduce power consumption, as demonstrated in previous examples, and to enable the deployment of novel sensor technologies. However, despite these advantages, ML-based approaches face several challenges. First, embedding synaptic weights directly into hardware in neuromorphic systems limits flexibility in weight adjustment compared to software-based approaches, hindering effective adaptation to long-term sensor degradation and signal drift. This limitation is especially critical, as the fixed nature of analog weights may require physical hardware modifications for any recalibration, ultimately leading to increased system maintenance costs. Second, most current applications of ML are optimized for specific scenarios, making performance susceptible to degradation when sensor specifications or environmental conditions vary. Addressing these limitations requires collecting training data under diverse conditions and increasing the depth of model layers and the number of nodes. However, this approach significantly raises data collection costs and complexity. As we move into the IoT era, it is crucial to explore innovative approaches to efficiently process and integrate the vast amounts of data generated by diverse sensors. With the continued advancement of ML technologies, it is expected that new applications will emerge, not only complementing the functionality of sensors but also fundamentally transforming how they operate.

3.6. Simultaneous Enhancement of Multiple Sensor Performance Metrics

In the previous sections, we discussed how ML has been used to enhance individual sensor parameters. However, the ultimate goal of integrating ML into sensor technologies is to simultaneously improve multiple metrics, leading to holistic performance gains. This section introduces examples addressing the persistent challenges of low selectivity and slow response speed in gas sensors, as well as cases in physical sensors where improvements in spatial resolution have been achieved in parallel with in-sensor computing to enhance practical applicability.

K. Lee developed a CNN-based e-nose system capable of simultaneously classifying gas species and predicting gas concentrations, including previously untrained levels (**Figure** 8a-i).[126] This approach contrasts with the system shown in Figure 3b, which could only classify mixed gases at predefined ratios. The system used two μLED gas sensors with different sensing materials, and the collected time-series response data were preprocessed using a sliding time window to generate 2D input matrices for CNN training. Classification labels ranged from 0 (normal air) to 4 (target gases), while regression labels were normalized by the maximum concentration to reduce training bias. To improve model generalization, artificial deviations of ±10% were added to the original responses as a form of data augmentation. This strategy is particularly useful in sensor systems where data collection is

© 2025 The Author(s). Advanced Functional Materials published by Wiley-VCH GmbH

16163028, 0, Downloaded from https://advanced.onlinelibrary.wiley.com/doi/10.1002/adfm.202519859 by Inkyu Park - Korea Advanced Institute Of , Wiley Online Library on [10/12/2025]. See the Terms and Conditions (https://onlinelibrary.wiley.com/terms-and-conditions) on Wiley Online Library for rules of use; OA articles are governed by the applicable Creative Commons License

16163028, 0, Downloaded from https://advanced.onlinelibrary.wiley.com/doi/10.1002/adfm.202519859 by Inkyu Park - Korea Advanced Institute Of , Wiley Online Library on [10/12/2025]. See the Terms and Conditions (https://onlinelibrary.wiley.com/terms-and-conditions) on Wiley Online Library for rules of use; OA articles are governed by the applicable Creative Commons License

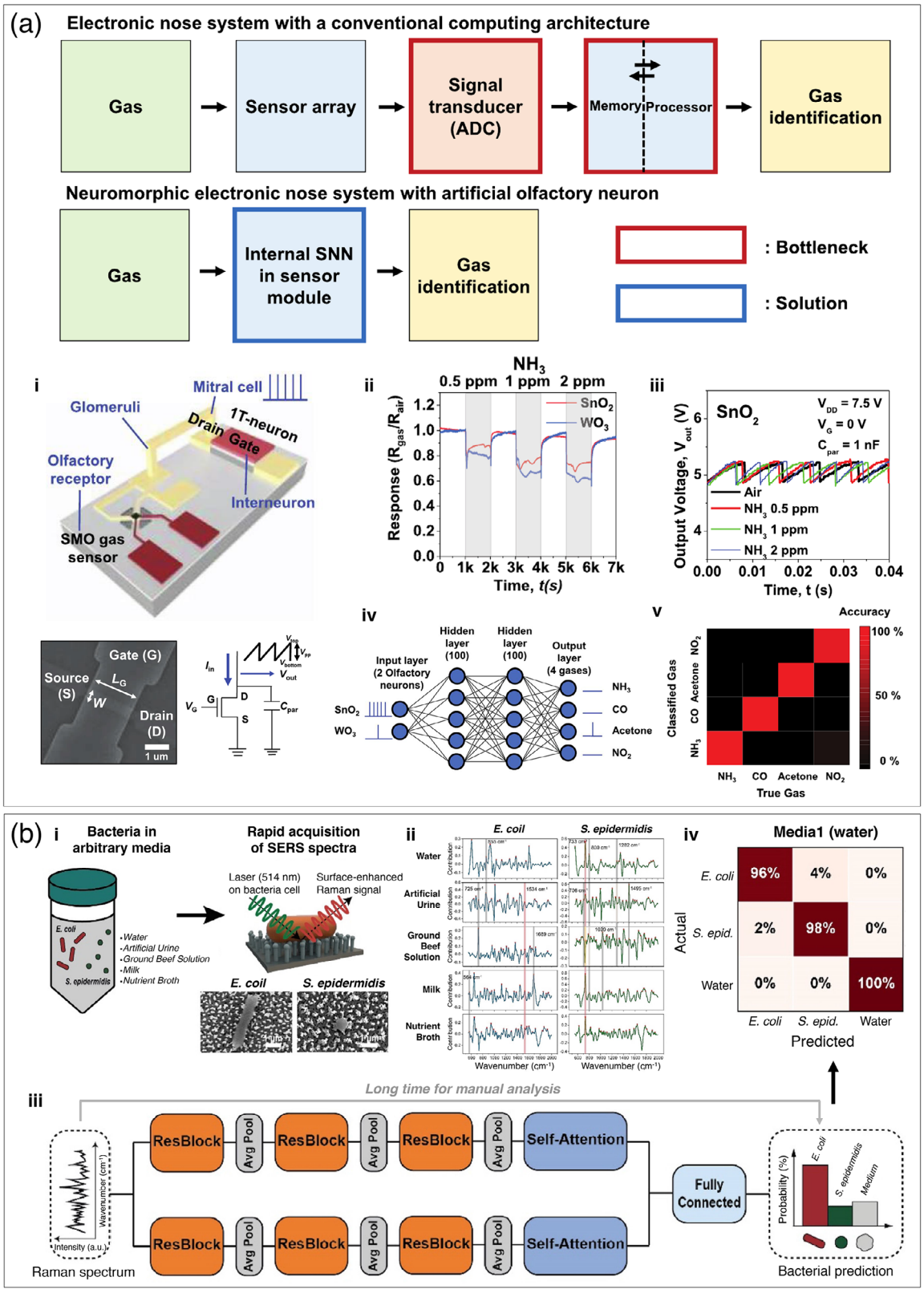

Figure 7. ML-Driven approaches to enhance power efficiency and enable automated analysis in practical sensor applications. a) E- nose system that utilizes neuromorphic computing to program neural networks into hardware, reducing power consumption by replacing ADCs and processors, reproduced under the terms of the CC-BY-4.0 license,[124] Copyright 2022, The Authors. Advanced Science published by Wiley-VCH GmbH b) Analysis algorithm that reduces analysis time to identify bacteria species by analyzing SERS signals instead of humans, reproduced with permission,[125] Copyright 2022, Elsevier B.V. All rights reserved.

© 2025 The Author(s). Advanced Functional Materials published by Wiley-VCH GmbH

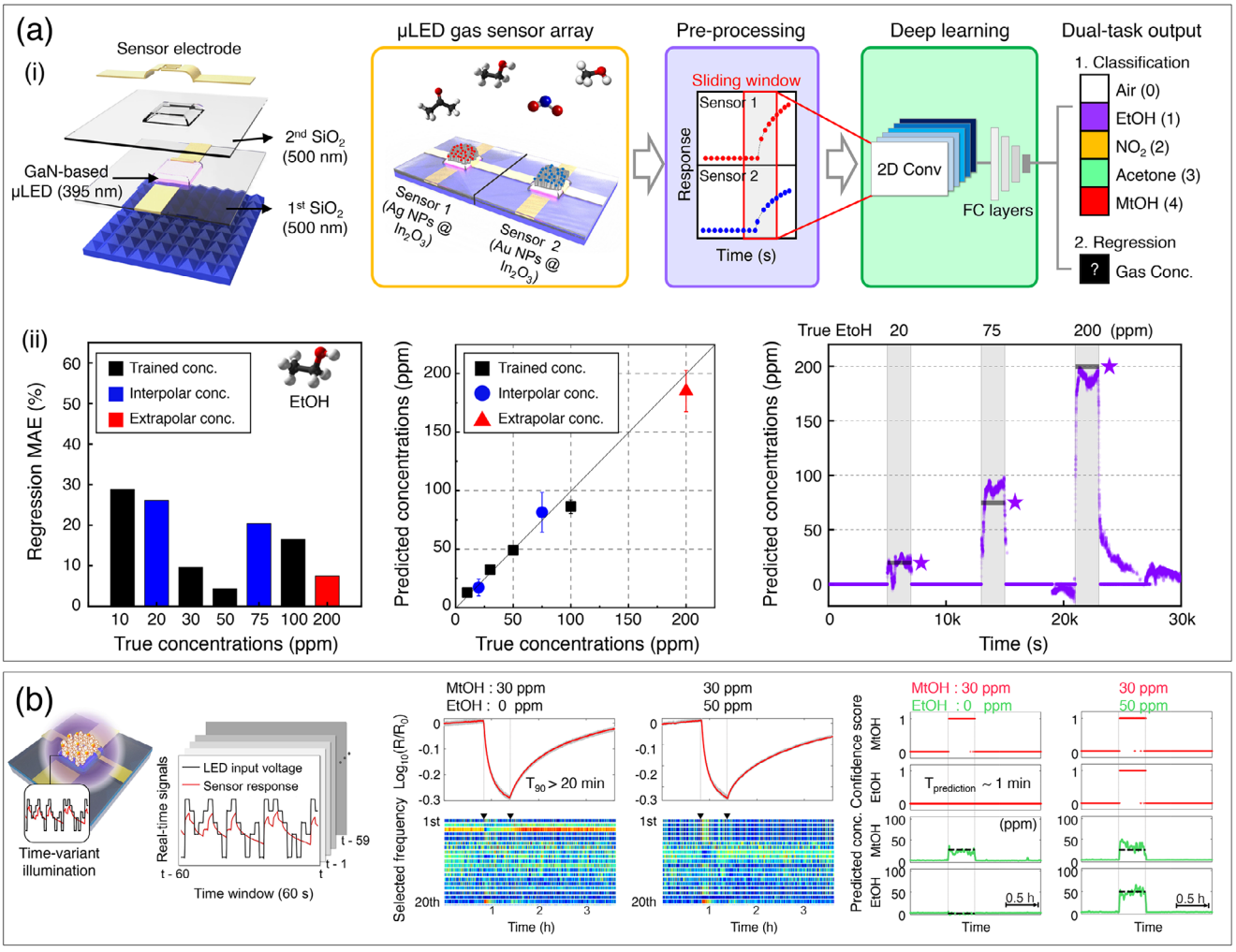

Figure 8. Simultaneous enhancement of multiple sensor performance metrics. a) Dual-task e-nose system using two sensors for simultaneous classification (99.32% accuracy) and regression (13.82% MAE), with interpolation and extrapolation of untrained ethanol concentrations, reproduced with permission,[126] Copyright 2023, American Chemical Society. b) Single μLED sensor with pseudo-random illumination and spectrogram-based CNN, enabling accurate identification of gases and mixtures with reduced prediction time and power consumption, reproduced under the terms of the CC-BY-4.0 license,[58] Copyright 2023, The Author(s).

time-consuming, though it requires sufficient sensor-to-sensor uniformity and reproducibility. The model achieved 99.3% classification accuracy across five gas classes and an MAE of 13.8% for concentration regression. Despite being trained only on 10, 30, 50, and 100 ppm ethanol concentrations, the model successfully predicted untrained concentrations at 20 and 75 ppm (interpolation) and 200 ppm (extrapolation), as shown in Figure 8a-ii. This was possible not because the model treated each gas mixture as a separate class label, as introduced in Section 3.1, but because it used a regression-based approach capable of estimating continuous concentration values. This result demonstrates that the integration of ML enabled simultaneous enhancement of selectivity and a broadened sensing range beyond the trained concentration levels.

Using the same μLED gas sensor platform, Cho et al. further advanced the system by achieving high selectivity for mixed gas detection using only a single sensor (Figure 8b).[58] The μLED was operated with a randomly varying illumination pattern, enabling each gas to leave a distinct footprint in the signal and thereby yielding high-dimensional sensor responses. These signals were then converted into spectrograms using the fast Fourier transform (FFT), which captured unique frequency components for each gas. These spectrograms were used as input data for CNN training, allowing accurate classification of gases in mixtures, even distinguishing between chemically similar ones like methanol and ethanol. Beyond enhancing selectivity under mixed conditions, collecting ML training data via unique sensor operation techniques and utilizing it through optimized data processing can further enable reductions in system size and power consumption. Additionally, in both case studies of μLED gas sensors, ML played a key role in accelerating response time. Photoactivated gas sensors operate at room temperature, so their response is slower than heating-based sensors, typically taking ≈10 min for full response and recovery. In this context, CNN models reduced the response time to within 1 min by leveraging early-stage transient signals.

© 2025 The Author(s). Advanced Functional Materials published by Wiley-VCH GmbH

16163028, 0, Downloaded from https://advanced.onlinelibrary.wiley.com/doi/10.1002/adfm.202519859 by Inkyu Park - Korea Advanced Institute Of , Wiley Online Library on [10/12/2025]. See the Terms and Conditions (https://onlinelibrary.wiley.com/terms-and-conditions) on Wiley Online Library for rules of use; OA articles are governed by the applicable Creative Commons License

In the field of physical and haptic sensors, there are cases where ML has been used to enhance spatial resolution, which has been simultaneously achieved through in-sensor computing as introduced in Section 3.5. To achieve high practicality and integration into daily life, it is essential to consider computing power and develop platforms where sensing and computation are tightly integrated. Such simultaneous enhancements in the physical sensor domain hold promise for future applications in human–computer interaction and password security.[127,128] These examples illustrate how ML can simultaneously enhance multiple sensor parameters, including selectivity, sensing range, energy and size efficiency, and response time, without modifying the sensor hardware. As sensor systems attempt to improve an increasing number of parameters simultaneously, computational cost and algorithmic complexity will inevitably rise. Therefore, it is crucial to carefully consider the intrinsic properties of the sensor signal data as well as the underlying sensing mechanism, and to select an appropriate ML model that aligns with these characteristics. Without this alignment, improving one metric may come at the expense of others, making it difficult to achieve balanced overall performance.

4. Applications of ML-Enhanced Sensors

ML has revolutionized the functionality and scope of sensors by enabling real-time, adaptive, and precise data processing. ML-enhanced sensors now play an indispensable role in various industries, addressing limitations in traditional sensor technologies, such as low accuracy, environmental interference, and high costs. This chapter delves into key applications of ML-integrated sensors across diverse domains, demonstrating how advancements in ML algorithms and sensor technologies synergize to unlock groundbreaking possibilities. The chapter begins by exploring human motion monitoring, highlighting its transformative impact on healthcare, virtual reality, and human–machine interfaces. Subsequent sections focus on innovative applications in environmental sensing, including e-nose systems for disease diagnosis and food monitoring. These applications exemplify the power of ML algorithm in amplifying sensor capabilities, enabling scalability, and paving the way for future innovations.

4.1. Human Motion Monitoring

The convergence of ML and sensor technology has significantly advanced human motion monitoring, enabling real-time analysis and adaptive response mechanisms in various applications such as healthcare, rehabilitation, and interactive digital environments. Among the diverse sensor technologies, soft sensors stand out for their remarkable adaptability in capturing complex motion data, while simultaneously providing enhanced user comfort during operation. Building on these advantages, ML algorithms are applied to effectively analyze and interpret the data obtained from soft sensors. Common ML methods utilized in motion monitoring include CNN for pattern recognition, LSTM networks for time-series motion tracking, and SVMs for classification tasks. Additionally, multilayer perceptrons (MLPs) and PCA play essential roles in feature extraction and dimensionality reduction. These techniques collectively enable high-accuracy motion detection, real-time adaptation, and scalable solutions across multiple fields. Recent breakthroughs in ML-powered motion monitoring include smart gloves for sign language recognition, soft sensor arrays for multimodal sensing, and haptic-feedback rings for immersive interactions. These innovations have enhanced the ability to track, analyze, and respond to human motion in real-time, making them indispensable for assistive technologies, AR/VR gaming, industrial automation, and rehabilitation monitoring. By integrating ML-driven predictive analytics and models, these sensor systems offer personalized feedback, gesture recognition, and interactive control, significantly expanding their usability and impact.

Sign language recognition has significantly benefited from ML-powered sensor systems. A notable example is a triboelectric smart glove that employs DNN models (CNNs and LSTMs) to recognize 50 words and 20 sentences with an accuracy of 91.3% and 95%, respectively (**Figure 9a**).[129] Additionally, the system enables real-time bidirectional communication in VR environments by converting gestures into comprehensible text and audio. This breakthrough enhances accessibility for speech and hearing-impaired individuals, making ML-enhanced sensors a crucial tool in assistive technology.

ML-powered wearable sensors have revolutionized gesture-based interactions in AR/VR environments and gaming.[130–133] Data gloves equipped with multiwalled carbon nanotube (MWCNT) sensors use hybrid CNN-LSTM models to achieve 97.5% accuracy in real-time gesture recognition, with an average processing time of 2.173 ms (Figure 9b).[134] These systems improve user experience in gaming and smart interfaces by enabling gesture-based control, robotic dexterity enhancement, and real-time interactions in virtual environments. On the other hand, bioinspired soft sensor arrays (BOSSA) integrate ML models (MLPs and SVMs) to enhance multimodal sensing, achieving 98.9% accuracy in user recognition and 98.6% accuracy in object identification (Figure 9c).[135]

Beyond these developments, next-generation intelligent sensor platforms have been reported that embed sensing and computing within the device architecture itself, reducing data redundancy and enhancing adaptability. Huang et al. introduced an in-device topological encoding interface that achieves one-channel multimodal fusion of touch and strain, enabling robotic arm control with >99% recognition accuracy.[128] Lin et al. demonstrated a programmable event-driven haptic interface with a gradient pyramid metasurface that improves sensitivity by 350% and supports real-time adaptive gesture recognition in AR/VR environments.[127] In a further development, Lin et al. proposed a bioinspired haptic interface modeled after the electric eel (Bio-EE). The design combines dielectrically modified polymers with optimized microstructures to decouple proximity and touch signals, extending detection up to 7 cm while maintaining high spatial resolution (500 μm).[136] These breakthroughs significantly expand the scope of ML-powered wearable systems for motion monitoring by enabling context-aware, proximity-enhanced, and self-adaptive sensing capabilities.

© 2025 The Author(s). Advanced Functional Materials published by Wiley-VCH GmbH

16163028, 0, Downloaded from https://advanced.onlinelibrary.wiley.com/doi/10.1002/adfm.202519859 by Inkyu Park - Korea Advanced Institute Of , Wiley Online Library on [10/12/2025]. See the Terms and Conditions (https://onlinelibrary.wiley.com/terms-and-conditions) on Wiley Online Library for rules of use; OA articles are governed by the applicable Creative Commons License

Figure 9. ML-enhanced Sensors for human motion monitoring. a) A triboelectric smart glove integrated with ML algorithms capable of reconstructing unseen sentences, enabling sign language translation and facilitating real-time communication in virtual reality environments, reproduced under the terms of the CC-BY-4.0 license,[129] Copyright 2021, The Author(s). b) A low-cost data glove employing a deep-learning hybrid CNN-LSTM model for gesture-based controls in smart vehicles, improving robotic dexterity, and supporting immersive interactions in virtual and augmented reality systems, reproduced under the terms of the CC-BY-4.0 license,[134] Copyright 2022 The Authors. Advanced Intelligent Systems, published by Wiley-VCH GmbH. c) Bioinspired triboelectric soft sensor arrays utilizing MLP for applications in industrial automation, smart home management, and rehabilitation monitoring, reproduced under the terms of the CC-BY-4.0 license,[135] Copyright 2022, American Chemical Society. d) Augmented Tactile-Perception and Haptic-Feedback Ring incorporating triboelectric and pyroelectric sensors for gesture recognition and temperature sensing, designed for use in metaverse applications, robotic systems, and rehabilitation therapies, reproduced under the terms of the CC-BY-4.0 license,[137] Copyright 2022, The Author(s).

© 2025 The Author(s). Advanced Functional Materials published by Wiley-VCH GmbH

16163028, 0, Downloaded from https://advanced.onlinelibrary.wiley.com/doi/10.1002/adfm.202519859 by Inkyu Park - Korea Advanced Institute Of , Wiley Online Library on [10/12/2025]. See the Terms and Conditions (https://onlinelibrary.wiley.com/terms-and-conditions) on Wiley Online Library for rules of use; OA articles are governed by the applicable Creative Commons License

16163028, 0, Downloaded from https://advanced.onlinelibrary.wiley.com/doi/10.1002/adfm.202519859 by Inkyu Park - Korea Advanced Institute Of , Wiley Online Library on [10/12/2025]. See the Terms and Conditions (https://onlinelibrary.wiley.com/terms-and-conditions) on Wiley Online Library for rules of use; OA articles are governed by the applicable Creative Commons License

4.2. Haptic Feedback

ML-driven haptic feedback systems significantly improve interactive experiences in virtual environments, robotic control, and medical training. A notable example is the Augmented Tactile-Perception and Haptic-Feedback Ring, which integrates triboelectric and pyroelectric sensors for real-time gesture recognition, tactile sensing, and temperature feedback (Figure 9d).[137] These compact, flexible devices use ML-based control to deliver vibro- and thermo-haptic responses, making them well-suited for metaverse applications, surgical simulations, and remote robotic operations.

The integration of ML with advanced sensor technology, especially soft sensors, has revolutionized human motion monitoring by enabling real-time, highly accurate analysis and adaptive response mechanisms. Notable innovations, including triboelectric smart gloves for sign language recognition, data gloves for AR/VR gesture control, and BOSSA for multimodal sensing, have demonstrated exceptional performance in accuracy. Moreover, ML-driven haptic feedback systems, such as the Augmented Tactile-Perception and Haptic-Feedback Ring, illustrate the potential for immersive and interactive experiences in virtual environments, medical training, and remote operations. However, significant challenges persist, including improving the scalability and generalizability of ML models to accurately recognize gestures across diverse populations and contexts. Further advancements in sensor miniaturization, ensuring sustained sensitivity and reliability under various environmental conditions, are crucial for broadening wearable device applicability and user acceptance. Finally, developing adaptive recalibration and personalized learning algorithms, will substantially increase the practicality, reliability, and user-centric effectiveness of ML-powered motion monitoring solutions.

4.3. Chemical Sensing for Disease Diagnosis

Integration of ML with environmental sensors, such as gas and electrochemical (pH, H_2O_2, ion) sensors, have shown promising results for advanced applications like industrial emission monitoring, disease diagnosis, detect illegal drugs, food spoilage monitoring, and plant stress monitoring.[138] Human breath contains a mixture of gases that can indicate health status, while food releases distinct aromas and VOC gases as it transitions from fresh to spoiled states. Similarly, plants emit substances in response to stress conditions, such as water deficiency, salinity, H_2O_2, or pH changes. These emissions are often present in trace amounts, highly complex, and composed of numerous mixed components. By integrating ML, it becomes possible to identify these complex patterns and significantly enhance the system's overall robustness and accuracy.

GeNose C19 is a non-invasive e-nose system designed for rapid COVID-19 screening through exhaled breath analysis (**Figure 10a**).[139] The system employs high-efficiency-particulate-air (HEPA) filters and 10 metal oxide semiconductor sensors to detect VOCs and classify positive and negative cases. Breath samples from 83 participants (43 COVID-19-positive, 40 negative) were collected in medical-grade bags to minimize contamination, with each sample analyzed 10 times for reliability. Data preprocessing included baseline normalization and feature extraction (e.g., maximum, median, standard deviation), resulting in 40 features per sample. Four ML models (LDA, SVM, MLP, and DNN) were tested, with DNN achieving the best performance: 95.5% sensitivity, 95.7% specificity, and an area under the curve (AUC) of 96.87%, thanks to optimized hyperparameters and 10-fold cross-validation. GeNose C19 enables fast (≈3 min), non-invasive, and cost-effective COVID-19 diagnostics, addressing limitations of reverse transcription-quantitative polymerase chain reaction. Future studies aim to validate the system with larger cohorts, identify key VOC biomarkers, and explore applications in other respiratory diseases, showcasing its scalability as a diagnostic tool.

4.4. Food Safety and Smart Farming

The Biomimetic Olfactory Chip (BOC) system integrates a high-density nanotube sensor array for VOC detection through chemiresistive sensing (Figure 10b).[140] Depending on the design, each BOC chip incorporates between 100 and 10 000 individual PdO/SnO_2 nanotube sensors. A multi-component interfacial layer was deposited on the PdO/SnO_2 layer using a specialized sputtering process. Owing to the 2D spatial gradient in the deposition of multiple metal oxides, each sensor in the array was coated with a distinct MCI composition. This straightforward approach enables the fabrication of a heterogeneous sensor array composed of different sensing materials, thereby enhancing selectivity and discrimination. The BOC system has been employed for single-gas discrimination of eight gases with different concentrations and humidity levels. It has also been applied to gas mixture deconvolution, analyzing four gases (ethanol, toluene, formaldehyde, and carbon monoxide) across 96 different mixtures. In addition, the system was used for food freshness monitoring, where VOC emissions from a sliced orange stored for nine days were analyzed. Initially, d-limonene was the dominant VOC, but as spoilage progressed, ethanol emissions increased. The system's chemiresistive sensors captured these changes through normalized 10×10 heatmaps. For ML analysis, a CNN was applied to classify gas response patterns by leveraging spatial features from the sensor array, and an SVM with a linear kernel was used to define decision boundaries. To further investigate odor distribution, t-distributed stochastic neighbor embedding (t-SNE) was used to reduce the 100D Euclidean distance into a 2D space. For single-gas discrimination, the optimized model reached a prediction accuracy of 99.04%. The authors also noted that while adding more sensors increases model accuracy and reliability, the improvements plateau beyond a certain threshold. They further pointed out that greater numbers and diversity of pixels can introduce data redundancy and demand more complex signal readout devices. Overall, this study highlights the potential of e-nose technology based on large-scale monolithic sensor arrays for real-time, non-invasive food quality assessment, and suggests that coupling such arrays with ML could pave the way for next-generation olfactory systems with enhanced selectivity and discrimination.

The Time-Resolved Electrochemical Technology for Plant Root Environment in Situ Chemical Sensing (TETRIS) system is a multi-sensor electrochemical platform designed to continuously

© 2025 The Author(s). Advanced Functional Materials published by Wiley-VCH GmbH

16163028, 0, Downloaded from https://advanced.onlinelibrary.wiley.com/doi/10.1002/adfm.202519859 by Inkyu Park - Korea Advanced Institute Of , Wiley Online Library on [10/12/2025]. See the Terms and Conditions (https://onlinelibrary.wiley.com/terms-and-conditions) on Wiley Online Library for rules of use; OA articles are governed by the applicable Creative Commons License

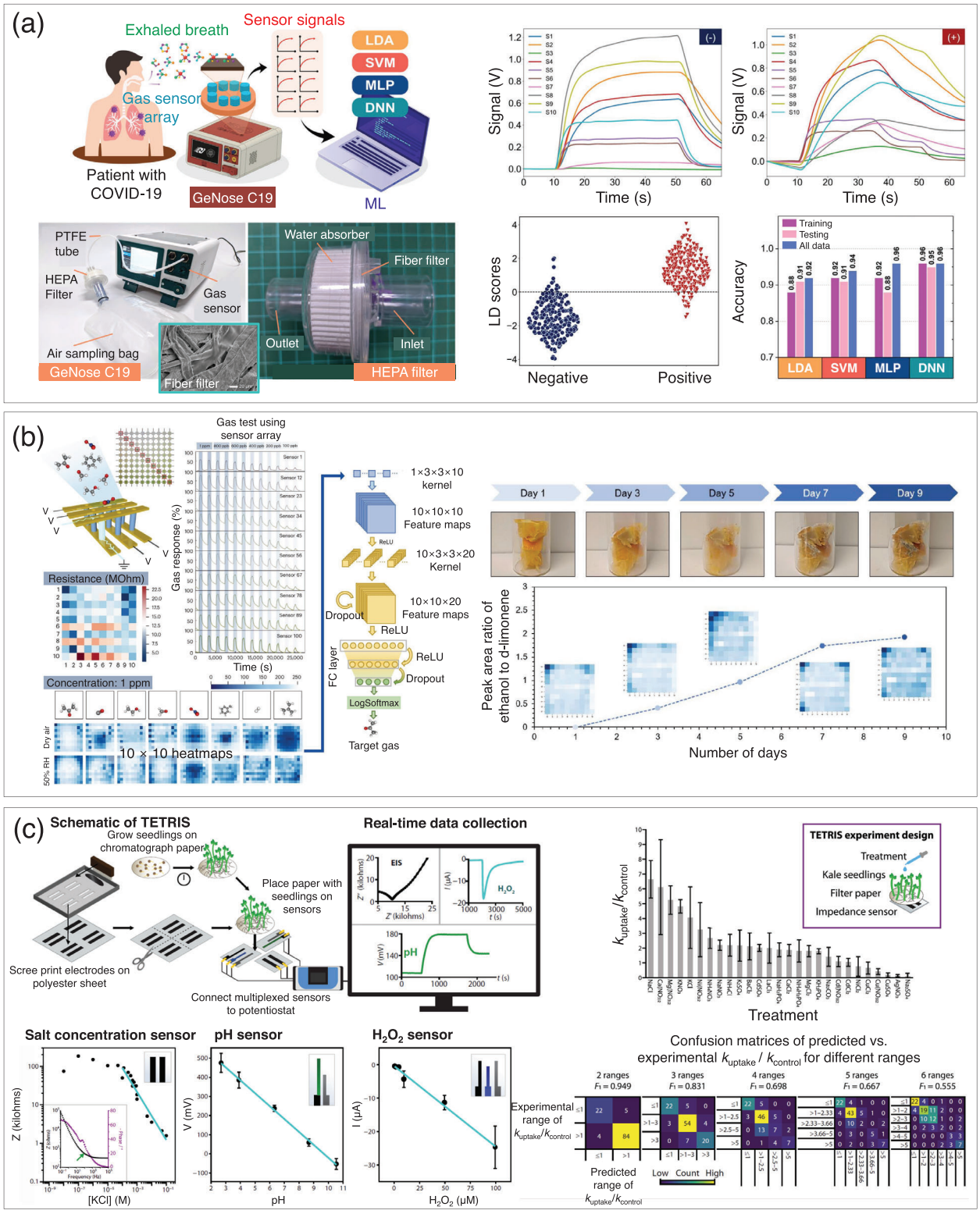

Figure 10. ML-enhanced environmental sensing for healthcare, food safety, and smart farming. a) ML-driven e-nose system for non-invasive COVID-19 screening through exhaled breath analysis, reproduced under the terms of the CC-BY-4.0 license,[139] Copyright 2022, The Author(s). b) VOC-based food spoilage monitoring, detecting ethanol emissions to assess freshness over time, reproduced with permission,[141] Copyright 2024, The Author(s), under exclusive license to Springer Nature Limited. c) Electrochemical sensor platform for real-time plant stress monitoring, analyzing key chemical markers in smart farming applications, reproduced under the terms of the CC-BY-4.0 license,[140] Copyright 2024, The American Association for the Advancement of Science.

© 2025 The Author(s). Advanced Functional Materials published by Wiley-VCH GmbH

monitor key chemical parameters in plant roots under stress conditions (Figure 10c).[141] It employs screen-printed electrochemical sensors to detect ion concentrations (K^+, Na^+, Ca^{2+}, NH^{4+}, Mg^{2+}), pH fluctuations, and reactive oxygen species (H_2O_2) in real-time—key indicators of plant physiological status under environmental stressors such as salinity, nutrient imbalance, or oxidative damage. To quantify plant-specific ion uptake dynamics, the authors introduced k_{uptake}, a parameter reflecting how ion concentration in the root environment changes over time. This value was normalized by $k_{control}$, a baseline uptake rate measured without plants, to correct for side effects like evaporation. A supervised ML framework based on XGBoost (gradient boosting–based decision tree algorithm) was employed to classify the normalized ion uptake ratio ($k_{uptake}/k_{control}$), using time-resolved electrochemical data and physicochemical properties of the ions (e.g., relative mass, charge state, and biological relevance to plants) as input features. The target variable was categorized into multiple levels, ranging from a binary classification (uptake vs no uptake) to more detailed 3–6 range models. The predicted categories were compared against experimentally measured values using confusion matrices, and the two-range model achieved a high F1 score of 0.949. This approach enabled the quantitative interpretation of ion transport behavior associated with plant stress responses and demonstrated the potential of integrating ML with sensor data for precision agriculture, optimized nutrient management, and early stress detection.

By combining ML with advanced sensors, we can now monitor gases and biomarkers from humans, animals, and plants, enabling applications in healthcare, food safety, and smart farming. Living organisms have complex metabolic processes, constantly producing and releasing various substances, making selectivity essential for accurate detection. Beyond merely classifying conditions as normal or abnormal, many applications require identifying the cause of abnormalities, highlighting the need for high diagnostic accuracy. To be practical, fast analysis time and low-power characteristics are also key for real-time monitoring. As sensor technology improves and more data is collected, stronger and more efficient ML models can be developed, making non-invasive, quick, and real-time biological monitoring increasingly feasible. These advancements will open new possibilities for smarter, faster, and more precise sensing solutions.

5. Challenges and Perspectives

While sensors integrated with ML are advancing significantly and are increasingly deployed across diverse applications, they still encounter substantial challenges that need resolution to propel further advancements in next-generation physical and chemical sensor technologies. Addressing these challenges is imperative as it opens up substantial potential for the evolution of sensor capabilities.

First, the substantial data requirement for training and validation remains a major challenge. Most ML models require extensive datasets, yet real-world data collection is often limited, as many studies are conducted in controlled laboratory settings where large-scale data generation is impractical. This limitation hinders the development of robust ML models that can generalize across different environments. To mitigate this issue, techniques such as data augmentation, transfer learning, and synthetic data generation can enhance model robustness and simulate real-world variability.

Second, the inherent limitations of sensor hardware often act as bottlenecks in ML applications. In particular, flexible and wearable sensors frequently suffer from durability and reliability issues, which directly impact ML model stability. Additionally, ensuring reproducibility across different sensors is critical for the effective deployment of ML models. Even if a model is trained on a well-curated dataset, it cannot be reliably applied to new sensors unless their outputs remain consistent. This variability arises from differences in fabrication processes, material properties, and environmental conditions, which can lead to performance discrepancies. To address these challenges, it is essential to develop high-performance sensor platforms with improved reproducibility and reliability, enabled by advances in materials science and nanotechnology. In parallel, inevitable variability that may still arise during fabrication can be mitigated through algorithmic approaches such as noise reduction, self-calibration, and error correction, to build more robust and reliable ML models.

Third, ML has fundamental limitations in interpreting physical phenomena. Unlike physics-based models, which are grounded in well-established theoretical principles, data-driven ML models function as black-box systems that rely solely on data patterns and statistical correlations. As a result, they struggle to adapt to untrained scenarios, for example, when sensor configurations are modified due to material changes, structural adjustments, or environmental variations. This makes ML-based sensor models vulnerable to performance degradation in unpredictable conditions, restricting their adaptability. Overcoming this challenge requires hybrid approaches that combine ML with physics-informed models, enabling self-adaptive learning frameworks that adjust dynamically to sensor modifications.

Fourth, high computational complexity remains a major constraint, particularly for low-power IoT and wearable devices. Many ML techniques, especially DNN models, require significant computational resources, making real-time applications challenging. To address this issue, optimized ML algorithms with reduced complexity should be developed through model quantization and knowledge distillation. Additionally, edge computing offers a promising solution by enabling on-device data processing, minimizing latency, and energy consumption. The development of dedicated ML hardware (e.g., neuromorphic chips, ML accelerators for sensors) could further enhance computational efficiency without compromising performance.

Fifth, a major challenge in the current research environment is the disjointed application of ML algorithms, where individual studies frequently employ arbitrary ML techniques. This method fails to provide a cohesive integration of ML technologies that are specifically tailored to meet the unique demands of each sensor type (such as strain sensors, gas sensors, biosensors) and their respective performance indices (such as selectivity, response time, reliability). Consequently, there is a crucial demand for a more structured strategy that systematically aligns ML algorithms with the specific types of sensors and their intended performance objectives through a comprehensive literature review like the goal of this Review Article.

Sixth, integrating ML at the system level, beyond just sensor data processing, can yield more effective solutions. Instead of treating ML as an isolated tool for processing sensor

© 2025 The Author(s). Advanced Functional Materials published by Wiley-VCH GmbH

16163028, 0, Downloaded from https://advanced.onlinelibrary.wiley.com/doi/10.1002/adfm.202519859 by Inkyu Park - Korea Advanced Institute Of , Wiley Online Library on [10/12/2025]. See the Terms and Conditions (https://onlinelibrary.wiley.com/terms-and-conditions) on Wiley Online Library for rules of use; OA articles are governed by the applicable Creative Commons License

16163028, 0, Downloaded from https://advanced.onlinelibrary.wiley.com/doi/10.1002/adfm.202519859 by Inkyu Park - Korea Advanced Institute Of , Wiley Online Library on [10/12/2025]. See the Terms and Conditions (https://onlinelibrary.wiley.com/terms-and-conditions) on Wiley Online Library for rules of use; OA articles are governed by the applicable Creative Commons License

signals, a neural network-based system approach that includes actuators, information processing, and multi-sensor fusion could significantly enhance overall system efficiency. Future research should explore multi-sensor ML architectures that optimize entire sensing-actuation pipelines, leading to more intelligent and adaptive sensor networks.

Seventh, other sensor parameters beyond those discussed in this Review remain underexplored. While calibration, standardization, stability against environmental variations, and multimodal signal integration are equally critical indices for practical applications, systematic ML studies directly targeting these aspects are still limited. Expanding ML approaches to address such parameters could establish a more comprehensive framework for sensor performance enhancement. Future efforts should therefore prioritize extending ML methodologies to these underrepresented indices, ultimately ensuring greater reliability and applicability in real-world environments.

Eighth, broader ethical, sustainability, and societal considerations must also be addressed. Current ML-driven sensor research often overlooks issues beyond technical performance, including limited transparency in data disclosure and model reproducibility, which raises ethical concerns regarding trust and accountability. Sustainability concerns, from the environmental costs of sensor production to the energy demands of ML training, are still largely overlooked. Economic and societal aspects are equally important, as the transition from laboratory prototypes to large-scale deployment must consider cost, accessibility, and potential inequities in real-world adoption. Furthermore, commercialization and scalability pose challenges in aligning cutting-edge ML methods with regulatory standards and public acceptance. Future research should therefore integrate ethical responsibility, sustainable design, economic feasibility, and societal impacts into the development of ML-enhanced sensors, ensuring that technological advances translate into trustworthy, equitable, and environmentally responsible applications.

In conclusion, while ML presents significant opportunities for enhancing next-generation sensors, addressing challenges related to data availability, sensor hardware reliability, computational efficiency, and standardization is essential. Especially, while ML offers powerful solutions to problems that were previously difficult or impossible to solve, it is not always the perfect answer. In engineering, a deep understanding of the physical mechanism may not be essential for practical problem-solving. However, for tasks that require scientific reasoning and interpretability, relying too much on data-driven ML approaches without clear explanations can introduce bias into the learning process. For example, building a highly accurate model from low-quality data, such as noisy signals or very limited samples, may learn unintended biases introduced during preprocessing or labeling, rather than true patterns. This can result in overfitting and misleading conclusions. Therefore, it is advisable to apply ML only after the sensor hardware achieves a certain level of consistent performance. Also, the design of the ML algorithm should be based on a clear understanding of the goal. Using overly complex models without a specific need can waste computational resources and time without improving results. Therefore, overcoming ML's inherent limitations in understanding physical phenomena and moving toward system-level ML integration will be crucial for long-term advancements. A multidisciplinary approach—spanning ML, sensor technology, materials science, and embedded computing—is required to fully unlock ML's potential in revolutionizing physical and chemical sensors. Additionally, strengthening collaborations between academia and industry can further support this effort by facilitating access to broader datasets and standardized manufacturing protocols, ultimately enhancing the scalability and generalizability of ML-integrated sensors. By addressing these challenges, the field can move toward more reliable, efficient, and scalable ML-integrated sensor technologies, paving the way for widespread real-world adoption.

6. Conclusion

In this review, we comprehensively examined the transformative impact of ML on next-generation physical and chemical sensors. By addressing fundamental limitations in traditional sensors, ML has enabled groundbreaking advancements across various domains. Through the integration of ML algorithms with novel sensor technologies, significant improvements have been achieved in optimizing critical performance indices, including selectivity, response time, spatial resolution, stability (drift), power consumption, and analysis process. The applications of ML-enhanced sensors span diverse fields, such as healthcare, environmental monitoring, and smart farming. Notable examples include human motion monitoring systems that leverage ML for real-time gesture recognition and rehabilitation tracking, as well as e-nose systems that facilitate early disease detection and food safety assessments.

Despite these advancements, several challenges remain. The development of robust ML models requires extensive and diverse datasets, which are often difficult to obtain outside controlled laboratory settings. Furthermore, the integration of ML with flexible and wearable sensors necessitates improvements in sensor fabrication reliability and computational efficiency. Additionally, ML's inherent limitations in interpreting physical phenomena pose challenges when adapting to untrained scenarios or modified sensor architectures. Beyond these, other sensor parameters such as calibration, standardization, stability against environmental variations, and multimodal signal integration remain underexplored, highlighting the need for systematic ML methodologies to directly address them. Furthermore, ethical, sustainability, and societal considerations, including transparency in data disclosure, energy demands of ML training, economic feasibility, and equitable large-scale deployment, must also be integrated into future sensor research. Addressing these issues requires a multidisciplinary approach, combining expertise in ML, materials science, sensor engineering, and embedded computing. Future research should focus on developing adaptive ML algorithms capable of processing diverse sensor data in real-time, optimizing energy consumption, and ensuring cost-effective scalability.

In conclusion, the fusion of ML and sensor technologies marks a paradigm shift in the development of intelligent sensing systems. Continued innovation in this field holds the potential to address critical global challenges, from personalized healthcare to sustainable environmental monitoring. By bridging the gap

© 2025 The Author(s). Advanced Functional Materials published by Wiley-VCH GmbH

between hardware limitations and computational advancements, ML-enhanced sensors are poised to play a pivotal role in shaping the future of sensor technology and its applications in daily life.

Acknowledgements

K.L., O.G., and Y.K. contributed equally to this work. This work was supported by the National Research Foundation of Korea (NRF) grant funded by the Korean government (MSIT, Nos. RS-2025-00523026 and 2021R1A2C3008742). The authorsalso thank our colleagues, Gandha Satria Adi, Jong-An Choi, Byeongmin Kang, Byung-Ho Kang, Jiwon Moon, and Incheol Cho, for their valuable comments and discussions during the revision process.

Conflict of Interest

The authors declare no conflict of interest.

Keywords

deep neural networks, internet of things, machine learning, smart sensors

Received: July 30, 2025
Revised: September 17, 2025
Published online:

[1] S. Selvaraj, S. Sundaravaradhan, *SN Appl. Sci.* **2019**, *2*, 139.
[2] H. Landaluce, L. Arjona, A. Perallos, F. Falcone, I. Angulo, F. Muralter, *Sensors* **2020**, *20*, 2495.
[3] M. A. A. Mamun, M. R. Yuce, *IEEE Sens. J.* **2019**, *19*, 7771.
[4] W. Li, M. Awais, W. Ru, W. Shi, M. Ajmal, S. Uddin, C. Liu, *Adv. Meteorol.* **2020**, *2020*, 8396164.
[5] F. Wen, T. He, H. Liu, H.-Y. Chen, T. Zhang, C. Lee, *Nano Energy* **2020**, *78*, 105155.
[6] K. Gulati, R. S. Kumar Boddu, D. Kapila, S. L. Bangare, N. Chandnani, G. Saravanan, *Mater Today Proc.* **2022**, *51*, 161.
[7] H. Yin, Y. Cao, B. Marelli, X. Zeng, A. J. Mason, C. Cao, *Adv. Mater.* **2021**, *33*, 2007764.
[8] Y. Du, J. Gu, S. Duan, J. Trueb, A. Tzavelis, H.-S. Shin, H. Arafa, X. Li, Y. Huang, A. N. Carr, C. R. Davies, J. A. Rogers, *Proc. Natl. Acad. Sci. USA* **2025**, *122*, 2501220122.
[9] W. Heng, S. Yin, J. Min, C. Wang, H. Han, E. S. Sani, J. Li, Y. Song, H. B. Rossiter, W. Gao, *Science (1979)* **2024**, *385*, 954.
[10] W. Kim, K. Lee, S. Choi, E. Park, G. Kim, J. Ha, Y. Kim, J. Jang, J. H. Oh, H. Kim, W. Jiang, J. Yoo, T. Kim, Y. Kim, K.-N. Kim, J. Hong, A. Javey, D. Rha, T.-W. Lee, K. Kang, G. Wang, C. Park, *Nat. Mater.* **2025**, *24*, 925.
[11] S.-R. Kim, Y. Zhan, N. Davis, S. Bellamkonda, L. Gillan, E. Hakola, J. Hiltunen, A. Javey, *Nat. Electron.* **2025**, *8*, 353.
[12] F. Serpush, M. B. Menhaj, B. Masoumi, B. Karasfi, *Comput. Intell. Neurosci.* **2022**, *2022*, 1391906.
[13] X. Wang, C. Zhu, M. Wu, J. Zhang, P. Chen, H. Chen, C. Jia, X. Liang, M. Xu, *Sens. Actuators A Phys.* **2022**, *344*, 113727.
[14] W. Yu, Y. Liu, T. Dillon, W. Rahayu, F. Mostafa, *IEEE Internet Things J.* **2022**, *9*, 2443.
[15] H. Kim, Y.-T. Kwon, H.-R. Lim, J.-H. Kim, Y.-S. Kim, W.-H. Yeo, *Adv. Funct. Mater.* **2021**, *31*, 2005692.
[16] J. Yin, R. Hinchet, H. Shea, C. Majidi, *Adv. Funct. Mater.* **2021**, *31*, 2007428.
[17] T.-H. Yang, J. R. Kim, H. Jin, H. Gil, J.-H. Koo, H. J. Kim, *Adv. Funct. Mater.* **2021**, *31*, 2008831.
[18] J. J. Kim, Y. Wang, H. Wang, S. Lee, T. Yokota, T. Someya, *Adv. Funct. Mater.* **2021**, *31*, 2009602.
[19] K. Wang, L. W. Yap, S. Gong, R. Wang, S. J. Wang, W. Cheng, *Adv. Funct. Mater.* **2021**, *31*, 2008347.
[20] J. Ahn, S. Padmajan Sasikala, Y. Jeong, J. G. Kim, J.-H. Ha, S. H. Hwang, S. Jeon, J. Choi, B.-H. Kang, J. Ahn, J.-H. Jeong, S. O. Kim, I. Park, *Adv. Fiber Mater.* **2024**, *6*, 1927.
[21] J. Ahn, J.-H. Ha, Y. Jeong, Y. Jung, J. Choi, J. Gu, S. H. Hwang, M. Kang, J. Ko, S. Cho, H. Han, K. Kang, J. Park, S. Jeon, J.-H. Jeong, I. Park, *Nat. Commun.* **2023**, *14*, 833.
[22] J.-H. Ha, Y. Jeong, J. Ahn, S. Hwang, S. Jeon, D. Kim, J. Ko, B. Kang, Y. Jung, J. Choi, H. Han, J. Gu, S. Cho, H. Kim, M. Bok, S. A. Park, J.-H. Jeong, I. Park, *Mater. Horiz.* **2023**, *10*, 4163.
[23] J. Gu, Y. Jung, J. Ahn, J. Ahn, J. Choi, B. Kang, Y. Jeong, J.-H. Ha, T. Kim, Y. Jung, J. Park, J. Jung, S. Ryu, I. Lee, I. Park, *Nano Energy* **2024**, *130*, 110124.
[24] H. Jang, J. Ahn, Y. Jeong, J.-H. Ha, J.-H. Jeong, M.-W. Oh, I. Park, Y. S. Jung, *Adv. Mater.* **2024**, *36*, 2408320.
[25] O. Gul, M. Song, C.-Y. Gu, J. Ahn, K. Lee, J. Ahn, H. J. Kim, T.-S. Kim, I. Park, *Nat. Commun.* **2025**, *16*, 1337.
[26] J. Ahn, J.-S. Kim, Y. Jeong, S. Hwang, H. Yoo, Y. Jeong, J. Gu, M. Mahato, J. Ko, S. Jeon, J.-H. Ha, H.-S. Seo, J. Choi, M. Kang, C. Han, Y. Cho, C. H. Lee, J.-H. Jeong, I.-K. Oh, I. Park, *Adv. Energy Mater.* **2022**, *12*, 2201341.
[27] O. Gul, M. Song, C.-Y. Gu, J. Ahn, K. Lee, T.-S. Kim, J. Ahn, H. J. Kim, I. Park, *Small* **2025**, *21*, 2410247.
[28] J. Ahn, Y. Jeong, M. Kang, J. Ahn, S. Padmajan Sasikala, I. Yang, J.-H. Ha, S. H. Hwang, S. Jeon, J. Gu, J. Choi, B.-H. Kang, S. O. Kim, S. Kim, J. Choi, J.-H. Jeong, I. Park, *Small* **2024**, *20*, 2311736.
[29] J. Ko, G. Kim, I. Kim, S. H. Hwang, S. Jeon, J. Ahn, Y. Jeong, J.-H. Ha, H. Heo, J.-H. Jeong, I. Park, J. Rho, *Adv. Sci.* **2024**, *11*, 2407045.
[30] J.-H. Ha, I. Yang, J. Ahn, S. Kang, Z.-J. Zhao, Y. Jeong, H. Je, J. Cheong, S. H. Hwang, S. Jeon, J.-H. Jeong, S. Kim, I. Park, *Adv. Funct. Mater.* **2024**, *34*, 2315028.
[31] J.-H. Ha, J. Ko, J. Ahn, Y. Jeong, J. Ahn, S. Hwang, S. Jeon, D. Kim, S. A. Park, J. Gu, J. Choi, H. Han, C. Han, B. Kang, B.-H. Kang, S. Cho, Y. J. Kwon, C. Kim, S. Choi, G.-D. Sim, J.-H. Jeong, I. Park, *Adv. Funct. Mater.* **2024**, *34*, 2401404.
[32] Y. K. Jo, S.-Y. Jeong, Y. K. Moon, Y.-M. Jo, J.-W. Yoon, J.-H. Lee, *Nat. Commun.* **2021**, *12*, 4955.
[33] M.-S. Jo, K.-H. Kim, J.-S. Lee, S.-H. Kim, J.-Y. Yoo, K.-W. Choi, B.-J. Kim, D.-S. Kwon, I. Yoo, J.-S. Yang, M.-K. Chung, S.-Y. Park, M.-H. Seo, J.-B. Yoon, *ACS Nano* **2023**, *17*, 23649.
[34] K.-H. Kim, M.-S. Jo, S.-H. Kim, B. Kim, J. Kang, J.-B. Yoon, M.-H. Seo, *Nat. Commun.* **2024**, *15*, 8761.
[35] M. Kim, S. Park, J. Ahn, J. W. Baek, D.-H. Kim, H. Shin, J. Ko, L. Song, C. Park, E. Shin, I.-D. Kim, *ACS Sens.* **2024**, *9*, 6492.
[36] H. Han, H. Park, S. Cho, S.-U. Lee, J. Choi, J.-H. Ha, J. Park, Y. Jung, H. Kim, J. Ahn, Y. J. Kwon, Y. S. Oh, M. Je, I. Park, *Small* **2024**, *20*, 2405493.
[37] S. Cho, H. Han, H. Park, S.-U. Lee, J.-H. Kim, S. W. Jeon, M. Wang, R. Avila, Z. Xi, K. Ko, M. Park, J. Lee, M. Choi, J.-S. Lee, W. G. Min, B.-J. Lee, S. Lee, J. Choi, J. Gu, J. Park, M. S. Kim, J. Ahn, O. Gul, C. Han, G. Lee, S. Kim, K. Kim, J. Kim, C.-M. Kang, J. Koo, et al., *npj Flexible Electron.* **2023**, *7*, 8.
[38] S. Cho, J.-H. Ha, J. Ahn, H. Han, Y. Jeong, S. Jeon, S. Hwang, J. Choi, Y. S. Oh, D. Kim, S. A. Park, D. Lee, J. Ahn, B. Kang, B.-H. Kang, J.-H. Jeong, I. Park, *Adv. Funct. Mater.* **2024**, *34*, 2316196.
[39] O. Gul, J. Kim, K. Kim, H. J. Kim, I. Park, *Adv. Mater. Technol.* **2024**, *9*, 2302134.
[40] B. Lee, J. Lee, H.-K. Lee, H. Park, M.-J. Kwack, D. Y. Kim, I. Park, S. Lim, D.-S. Lee, *ACS Sens.* **2025**, *10*, 2510.

© 2025 The Author(s). Advanced Functional Materials published by Wiley-VCH GmbH

16163028, 0, Downloaded from https://advanced.onlinelibrary.wiley.com/doi/10.1002/adfm.202519859 by Inkyu Park - Korea Advanced Institute Of , Wiley Online Library on [10/12/2025]. See the Terms and Conditions (https://onlinelibrary.wiley.com/terms-and-conditions) on Wiley Online Library for rules of use; OA articles are governed by the applicable Creative Commons License

[41] B. Lee, M. Kang, K. Lee, Y. Chae, K.-J. Yoon, D.-S. Lee, I. Park, *ACS Sens.* **2025**, *10*, 954.
[42] J. Choi, C. Han, D. Lee, H. Kim, G. Lee, J.-H. Ha, Y. Jeong, J. Ahn, H. Park, H. Han, S. Cho, J. Gu, I. Park, *Sci. Adv.* **2025**, *11*, adv0057.
[43] K. Kim, J. Ahn, Y. Jeong, J. Choi, O. Gul, I. Park, *Micro Nano Syst. Lett.* **2021**, *9*, 2.
[44] H. Park, K. Kim, S.-J. Kweon, O. Gul, J. Choi, Y. S. Oh, I. Park, M. Je, *IEEE Trans Biomed Circuits Syst.* **2023**, *17*, 889.
[45] J. Ahn, T. Kim, J.-H. Ha, D. Lee, O. Gul, S. Cho, H. Kim, M. Kang, J. Choi, J. Ahn, I. Park, *Adv. Funct. Mater.* **2025**, *35*, 2502568.
[46] L. Wu, J. Ahn, J. Choi, J. Gu, X. Li, O. Gul, Z.-J. Zhao, L. Qian, B. Yu, I. Park, *Nano Energy* **2023**, *109*, 108299.
[47] O. Gul, K. Kim, J. Gu, J. Choi, D. Del Orbe Henriquez, J. Ahn, I. Park, *ACS Appl. Electron. Mater.* **2021**, *3*, 4027.
[48] A. Turlybekuly, Y. Shynybekov, B. Soltabayev, G. Yergaliuly, A. Mentbayeva, *ACS Sens.* **2024**, *9*, 6358.
[49] N. M. Vuong, N. D. Chinh, B. T. Huy, Y.-I. Lee, *Sci. Rep.* **2016**, *6*, 26736.
[50] I. Cho, Y. C. Sim, M. Cho, Y.-H. Cho, I. Park, *ACS Sens.* **2020**, *5*, 563.
[51] M. S. Kim, Y. Lee, J. Ahn, S. Kim, K. Kang, H. Lim, B.-S. Bae, I. Park, *Adv. Funct. Mater.* **2023**, *33*, 2208792.
[52] Z.-J. Zhao, J. Ahn, S. H. Hwang, J. Ko, Y. Jeong, M. Bok, H.-J. Kang, J. Choi, S. Jeon, I. Park, J.-H. Jeong, *ACS Nano* **2021**, *15*, 503.
[53] S. C. Mukhopadhyay, S. K. S. Tyagi, N. K. Suryadevara, V. Piuri, F. Scotti, S. Zeadally, *IEEE Sens. J.* **2021**, *21*, 24920.
[54] Z. Zhou, K. Chen, X. Li, S. Zhang, Y. Wu, Y. Zhou, K. Meng, C. Sun, Q. He, W. Fan, E. Fan, Z. Lin, X. Tan, W. Deng, J. Yang, J. Chen, *Nat. Electron.* **2020**, *3*, 571.
[55] M. A. Alsheikh, S. Lin, D. Niyato, H.-P. Tan, *IEEE Commun. Surv. Tutorials* **2014**, *16*, 1996.
[56] L. Liu, C. Hu, T. Ou, Z. Wang, Y. Zhu, N. Na, *Adv. Intell. Syst.* **2023**, *5*, 2200136.
[57] M. Kang, I. Cho, J. Park, J. Jeong, K. Lee, B. Lee, D. Del Orbe Henriquez, K. Yoon, I. Park, *ACS Sens.* **2022**, *7*, 430.
[58] I. Cho, K. Lee, Y. C. Sim, J.-S. Jeong, M. Cho, H. Jung, M. Kang, Y.-H. Cho, S. C. Ha, K.-J. Yoon, I. Park, *Light Sci. Appl.* **2023**, *12*, 95.
[59] M. G. Kim, M. Jue, K. H. Lee, E. Y. Lee, Y. Roh, M. Lee, H. J. Lee, S. Lee, H. Liu, B. Koo, Y. O. Jang, E. Y. Kim, Q. Zhen, S.-H. Kim, J. K. Kim, Y. Shin, *ACS Nano* **2023**, *17*, 18332.
[60] A. Ettalibi, A. Elouadi, A. Mansour, *Procedia. Comput. Sci.* **2024**, *231*, 212.
[61] Z. Su, B. L. Bentley, D. McDonnell, J. Ahmad, J. He, F. Shi, K. Takeuchi, A. Cheshmehzangi, C. P. da Veiga, *J. Med. Internet Res.* **2022**, *24*, 30503.
[62] T. M. Mitchell, *The Discipline of Machine Learning*, Carnegie Mellon University, Pittsburgh, USA **2006**.
[63] P. Domingos, *Commun. ACM* **2012**, *55*, 78.
[64] R. J. Rath, S. Farajikhah, F. Oveissi, F. Dehghani, S. Naficy, *Adv. Eng. Mater.* **2023**, *25*, 2200830.
[65] M. Penza, G. Cassano, *Sens Actuators B Chem* **2003**, *89*, 269.
[66] M. Pardo, G. Sberveglieri, *Sens Actuators B Chem* **2005**, *107*, 730.
[67] Y. Lu, D. Kong, G. Yang, R. Wang, G. Pang, H. Luo, H. Yang, K. Xu, *Adv. Sci.* **2023**, *10*, 2303949.
[68] K. Kumari, R. Parray, Y. B. Basavaraj, S. Godara, I. Mani, R. Kumar, T. Khura, S. Sarkar, R. Ranjan, H. Mirzakhaninafchi, *J Field Robot* **2025**, *42*, 5.
[69] Y. J. Hwang, H. Yu, G. Lee, I. Shackery, J. Seong, Y. Jung, S.-H. Sung, J. Choi, S. C. Jun, *Microsyst. Nanoeng.* **2023**, *9*, 28.
[70] D. V. D. O. Henriquez, M. Kang, I. Cho, J. Choi, J. Park, O. Gul, J. Ahn, D.-S. Lee, I. Park, *Small Methods* **2023**, *7*, 2201352.
[71] G. Yang, R. Song, Y. Wu, J. Yu, J. Zhang, H. Zhu, *IEEE Sens. J.* **2023**, *23*, 23753.
[72] Z. Feng, F. Wu, L. Zhao, *IEEE Sens. J.* **2024**, *24*, 6482.
[73] C. Park, J. Woo, M. Jeon, J. W. Baek, E. Shin, J. Kim, S. Park, I.-D. Kim, *ACS Nano* **2025**, *19*, 11230.
[74] K. B. Kim, M. S. Sohn, I.-S. Hwang, D. J. Yoo, S.-Y. Jeong, Y. C. Kang, Y. K. Moon, *Nat. Commun.* **2025**, *16*, 5121.
[75] P. M. Bulemo, D.-H. Kim, H. Shin, H.-J. Cho, W.-T. Koo, S.-J. Choi, C. Park, J. Ahn, A. T. Güntner, R. M. Penner, I.-D. Kim, *Chem. Rev.* **2025**, *125*, 4111.
[76] Y. Zhang, G.-X. Qi, Y.-L. Yu, M.-X. Liu, S. Chen, *Chem. Commun.* **2023**, *59*, 7603.
[77] S. Jobst, P. Recum, Á. Écija-Arenas, E. Moser, R. Bierl, T. Hirsch, *ACS Sens.* **2023**, *8*, 3530.
[78] J. Zhang, P. Srivatsa, F. H. Ahmadzai, Y. Liu, X. Song, A. Karpatne, Z. (James) Kong, B. N. Johnson, *Biosens. Bioelectron.* **2024**, *246*, 115829.
[79] V. Martvall, H. Klein Moberg, A. Theodoridis, D. Tomeček, P. Ekborg-Tanner, S. Nilsson, G. Volpe, P. Erhart, C. Langhammer, *ACS Sens.* **2025**, *10*, 376.
[80] Y. Kwon, K. Lee, M. Kang, C. Kim, J. H. Ha, H. Han, S. Yang, D. Yang, J. H. Seo, I. Park, *Sens Actuators B Chem* **2025**, *422*, 136693.
[81] S. Ando, E. Suzuki, *Knowl. Inf. Syst.* **2016**, *46*, 449.
[82] O. Casas, F. I. Rillo, *Rev. Sci. Instrum.* **2009**, *80*, 085102.
[83] N. S. S. Capman, X. V. Zhen, J. T. Nelson, V. R. S. K. Chaganti, R. C. Finc, M. J. Lyden, T. L. Williams, M. Freking, G. J. Sherwood, P. Bühlmann, C. J. Hogan, S. J. Koester, *ACS Nano* **2022**, *16*, 19567.
[84] R. Faleh, M. Othman, A. Kachouri, K. Aguir, *2014 1st Int. Conf. on Adv. Technologies for Signal and Image Processing, ATSIP 2014*, Sousse, Tunisia, March, **2014**, pp. 322–327.
[85] B. N. Johnson, R. Mutharasan, *Anal. Chem.* **2012**, *84*, 10426.
[86] C. B. Collins, J. M. Beck, S. M. Bridges, J. A. Rushing, S. J. Graves, *Proc. of the 1st Workshop on Artificial Intelligence and Deep Learning for Geographic Knowledge Discovery*, New York, USA, November, **2017**, pp. 37–44.
[87] J. Kędzierski, A. Rusiecki, *Procedia. Comput. Sci.* **2024**, *246*, 1250.
[88] A. Rezaei, M. C. Stevens, A. Argha, A. Mascheroni, A. Puiatti, N. H. Lovell, *IEEE Trans. Biomed. Eng.* **2023**, *70*, 115.
[89] P. L. Suárez, D. Carpio, A. D. Sappa, *Neurocomputing* **2024**, *573*, 127197.
[90] P. Wang, B. Bayram, E. Sertel, *Earth Sci. Rev.* **2022**, *232*, 104110.
[91] A. Bakhtiarnia, Q. Zhang, A. Iosifidis, *ACM Comput. Surv.* **2024**, *56*, 1.
[92] A. N. Wilson, K. A. Gupta, B. H. Koduru, A. Kumar, A. Jha, L. R. Cenkeramaddi, *IEEE Sens. J.* **2023**, *23*, 3395.
[93] M. C. Öz, T. S. Navruz, *2024 32nd Signal Processing and Communications Applications Conf. (SIU)*, Mersin, Turkey, May, **2024**, pp. 1–4.
[94] K. Minakawa, K. Ohta, H. Komatsu, T. Fukuyama, T. Ikuno, *AIP Adv.* **2024**, *14*, 015210.
[95] D. Kim, Y.-L. Park, *2018 IEEE/RSJ Int. Conf. on Intelligent Robots and Systems (IROS)*, Madrid, Spain, October, **2018**, pp. 7480–7485.
[96] S. Han, T. Kim, D. Kim, Y.-L. Park, S. Jo, *IEEE Robot. Autom. Lett.* **2018**, *3*, 873.
[97] C. Wei, S. Yu, Y. Meng, Y. Xu, Y. Hu, Z. Cao, Z. Huang, L. Liu, Y. Luo, H. Chen, Z. Chen, Z. Zhang, L. Wang, Z. Zhao, Y. Zheng, Q. Liao, X. Liao, *Adv. Mater.* **2025**, *37*, 2420501.
[98] S. Yu, Y. Xu, Z. Cao, Z. Huang, H. Wang, Z. Yan, C. Wei, Z. Guo, Z. Chen, Y. Zheng, Q. Liao, X. Liao, Y. Zhang, *Adv. Funct. Mater.* **2025**, *35*, 2416984.
[99] Z. Huang, S. Yu, Y. Xu, Z. Cao, J. Zhang, Z. Guo, T. Wu, Q. Liao, Y. Zheng, Z. Chen, X. Liao, *Adv. Mater.* **2024**, *36*, 2407329.
[100] N. Pesce, M. Fortunato, A. Tamburrano, *IEEE Sens. Lett.* **2023**, *7*, 1.
[101] T. Zhang, M. Zhao, M. Zhai, L. Wang, X. Ma, S. Liao, X. Wang, Y. Liu, D. Chen, *ACS Appl. Mater. Interfaces* **2024**, *16*, 11013.
[102] D. Badawi, A. Agambayev, S. Ozev, A. E. Cetin, *IEEE Sens. J.* **2021**, *21*, 17984.

© 2025 The Author(s). Advanced Functional Materials published by Wiley-VCH GmbH

16163028, 0, Downloaded from https://advanced.onlinelibrary.wiley.com/doi/10.1002/adfm.202519859 by Inkyu Park - Korea Advanced Institute Of , Wiley Online Library on [10/12/2025]. See the Terms and Conditions (https://onlinelibrary.wiley.com/terms-and-conditions) on Wiley Online Library for rules of use; OA articles are governed by the applicable Creative Commons License

[103] N. Mao, J. Xu, J. Li, H. He, *Math. Probl. Eng.* **2021**, https://doi.org/10.1155/2021/1636001.
[104] Y. Heng, Y. Zhou, D. H. Nguyen, V. D. Nguyen, M. Jiao, *Sens Actuators B Chem* **2025**, *422*, 136642.
[105] Y. Zhang, H. Zhao, J. Ma, Y. Zhao, Y. Dong, J. Ai, *Int. J. Aerosp. Eng.* **2021**, https://doi.org/10.1155/2021/3936826.
[106] Y. Oh, J. Lee, S. Kim, *Qual. Reliab. Eng. Int.* **2023**, *39*, 2422.
[107] M. Pereira, B. Glisic, *Expert Syst. Appl.* **2023**, *213*, 118884.
[108] S. Kwon, J. H. Park, H. D. Jang, H. Nam, D. E. Chang, *Appl. Sci.* **2024**, *14*, 2604.
[109] L. Feng, H. Dai, X. Song, J. Liu, X. Mei, *Sens Actuators B Chem* **2022**, *351*, 130986.
[110] X. Dong, S. Han, A. Wang, K. Shang, *Chemosensors* **2021**, *9*, 353.
[111] T. Chaudhuri, M. Wu, Y. Zhang, P. Liu, X. Li, *IEEE Sens. J.* **2021**, *21*, 7908.
[112] D. Pau, W. Ben Yahmed, F. M. Aymone, G. D. Licciardo, P. Vitolo, *Electronics* **2023**, *12*, 1.
[113] J. Payette, F. Vaussenat, S. Cloutier, *Sci. Rep.* **2023**, *13*, 11237.
[114] W. Guo, S. Yamagishi, L. Jing, *IEEE Access* **2024**, *12*, 18821.
[115] P. Khatri, K. K. Gupta, R. K. Gupta, *J. Ambient Intell. Humaniz. Comput.* **2021**, *12*, 3091.
[116] Z. Xu, J. Wang, Q. Fan, P. D. Lund, J. Hong, *J. Energy Storage* **2020**, *32*, 101678.
[117] D.-H. Shin, H.-J. Kim, *Structures* **2024**, *60*, 105875.
[118] L. Yang, X. Liu, W. Zhu, L. Zhao, G. C. Beroza, *Sci. Adv.* **2025**, *8*, abl3564.
[119] G. Muscogiuri, C. Martini, M. Gatti, S. Dell'Aversana, F. Ricci, M. Guglielmo, A. Baggiano, L. Fusini, A. Bracciani, S. Scafuri, D. Andreini, S. Mushtaq, E. Conte, P. Gripari, A. D. Annoni, A. Formenti, M. E. Mancini, L. Bonfanti, A. I. Guaricci, M. A. Janich, M. G. Rabbat, G. Pompilio, M. Pepi, G. Pontone, *Int. J. Cardiol.* **2021**, *343*, 164.
[120] F. Lacy, A. Ruiz-Reyes, A. Brescia, *Pattern Recognit. Lett.* **2024**, *179*, 115.
[121] L. Mennel, J. Symonowicz, S. Wachter, D. K. Polyushkin, A. J. Molina-Mendoza, T. Mueller, *Nature* **2020**, *579*, 62.
[122] F. Zhou, Y. Chai, *Nat. Electron.* **2020**, *3*, 664.
[123] Z. Ren, Z. Zhang, Y. Zhuge, Z. Xiao, S. Xu, J. Zhou, C. Lee, *Nanomicro Lett.* **2025**, *17*, 261.
[124] J.-K. Han, M. Kang, J. Jeong, I. Cho, J.-M. Yu, K.-J. Yoon, I. Park, Y.-K. Choi, *Adv. Sci.* **2022**, *9*, 2106017.
[125] E. Rho, M. Kim, S. H. Cho, B. Choi, H. Park, H. Jang, Y. S. Jung, S. Jo, *Biosens. Bioelectron.* **2022**, *202*, 113991.
[126] K. Lee, I. Cho, M. Kang, J. Jeong, M. Choi, K. Y. Woo, K.-J. Yoon, Y.-H. Cho, I. Park, *ACS Nano* **2023**, *17*, 539.
[127] W. Lin, Y. Xu, S. Yu, H. Wang, Z. Huang, Z. Cao, C. Wei, Z. Chen, Z. Zhang, Z. Zhao, Q. Liao, Y. Zheng, X. Liao, *Adv. Funct. Mater.* **2025**, *35*, 2500633.
[128] Z. Huang, H. Chen, Y. Luo, X. Xiao, S. Yu, L. Liu, Y. Hu, H. Wang, W. Lin, J. Zheng, Z. Guo, R. Gao, H. Yang, X. Zhu, Q. Liao, Y. Zheng, Z. Chen, X. Liao, *Adv. Funct. Mater.* **2025**, https://advanced.onlinelibrary.wiley.com/doi/full/10.1002/adfm.202515750.
[129] F. Wen, Z. Zhang, T. He, C. Lee, *Nat. Commun.* **2021**, *12*, 5378.
[130] S. Zhang, L. Suresh, J. Yang, X. Zhang, S. C. Tan, *Adv. Intell. Syst.* **2022**, *4*, 2100194.
[131] Z. Zhang, F. Wen, Z. Sun, X. Guo, T. He, C. Lee, *Adv. Intell. Syst.* **2022**, *4*, 2100228.
[132] M. Zhu, Z. Sun, Z. Zhang, Q. Shi, T. Chen, H. Liu, C. Lee, *2020 IEEE 33rd Int. Conf. on Micro Electro Mechanical Systems (MEMS)*, Vancouver, Canada, January, **2020**, pp. 16–19.
[133] J. Oh, S. Kim, S. Lee, S. Jeong, S. H. Ko, J. Bae, *Adv. Funct. Mater.* **2021**, *31*, 2170285.
[134] Y. Li, L. Yang, Z. He, Y. Liu, H. Wang, W. Zhang, L. Teng, D. Chen, G. Song, *Adv. Intell. Syst.* **2022**, *4*, 2200128.
[135] Y. Luo, X. Xiao, J. Chen, Q. Li, H. Fu, *ACS Nano* **2022**, *16*, 6734.
[136] W. Lin, H. Wang, R. Wangyuan, Y. Luo, G. Chen, S. Yu, L. Liu, Z. Huang, Y. Lin, Z. Guo, Y. Zheng, Z. Chen, X. Liao, *Adv. Funct. Mater.* **2025**, *35*, 2505912.
[137] Z. Sun, M. Zhu, X. Shan, C. Lee, *Nat. Commun.* **2022**, *13*, 5224.
[138] S. Huang, A. Croy, L. A. Panes-Ruiz, V. Khavrus, V. Bezugly, B. Ibarlucea, G. Cuniberti, *Adv. Intell. Syst.* **2022**, *4*, 2200016.
[139] D. K. Nurputra, A. Kusumaatmaja, M. S. Hakim, S. N. Hidayat, T. Julian, B. Sumanto, Y. Mahendradhata, A. M. I. Saktiawati, H. S. Wasisto, K. Triyana, *NPJ Digit Med.* **2022**, *5*, 115.
[140] C. Wang, Z. Chen, C. L. J. Chan, Z. Wan, W. Ye, W. Tang, Z. Ma, B. Ren, D. Zhang, Z. Song, Y. Ding, Z. Long, S. Poddar, W. Zhang, Z. Wan, F. Xue, S. Ma, Q. Zhou, G. Lu, K. Liu, Z. Fan, *Nat. Electron.* **2024**, *7*, 157.
[141] P. Coatsworth, Y. Cotur, A. Naik, T. Asfour, A. S.-P. Collins, S. Olenik, Z. Zhou, L. Gonzalez-Macia, D.-Y. Chao, T. Bozkurt, F. Güder, *Sci. Adv.* **2025**, *10*, adj6315.
[142] H. W. Noh, Y. Jang, H. D. Park, D. Kim, J. H. Choi, C.-G. Ahn, *Sens Actuators B Chem* **2023**, *390*, 133965.

Kichul Lee received his B.S. and M.S. degrees in Mechanical Engineering from KAIST in 2020 and 2022, respectively. He is currently a Ph.D. student in the Machine Intelligence & Novel Sensor Technology (MINT) research group at KAIST in the Mechanical Engineering Department since 2022. His research focuses on the development of semiconductor device fabrication, micro-LED-based photoactivated gas sensors, micro- and nanoscale materials science, and machine learning.

© 2025 The Author(s). Advanced Functional Materials published by Wiley-VCH GmbH

16163028, 0, Downloaded from https://advanced.onlinelibrary.wiley.com/doi/10.1002/adfm.202519859 by Inkyu Park - Korea Advanced Institute Of , Wiley Online Library on [10/12/2025]. See the Terms and Conditions (https://onlinelibrary.wiley.com/terms-and-conditions) on Wiley Online Library for rules of use; OA articles are governed by the applicable Creative Commons License

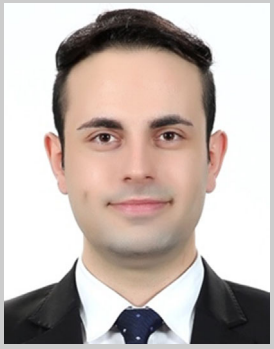

Osman Gul obtained his B.S. and M.S. degrees in Mechanical Engineering from Korea University and KAIST in 2019 and 2022, respectively. Currently, he is a Ph.D. candidate in the Mechanical Engineering Department at KAIST, working within the Machine Intelligence & Novel Sensor Technology (MINT) research group since 2022. His research focuses on flexible and stretchable electronics, liquid metals, soft material-based sensors, and applying machine learning to sensor technology.

Yeongjae Kwon obtained his B.S. and M.S. degrees in Mechanical Engineering from Yonsei University and KAIST in 2021 and 2023, respectively. Currently, he is a Ph.D. candidate in the Mechanical Engineering Department at KAIST, working within the Machine Intelligence & Novel Sensor Technology (MINT) research group since 2021. His research focuses on macro/nano fabrication, metal oxide gas sensor, machine learning, and IoT technology.

Ali Javey is the Lam Research Distinguished Chair in Semiconductor Processing and a professor of Electrical Engineering and Computer Sciences (EECS), and Materials Science and Engineering (MSE) at UC Berkeley. He is also a senior faculty scientist at the Lawrence Berkeley National Laboratory, where he serves as the program leader of Electronic Materials (E-Mat). He is a co-director of Berkeley Sensor and Actuator Center (BSAC). Javey received a Ph.D. degree in chemistry from Stanford University in 2005 and was a Junior Fellow of the Harvard Society of Fellows from 2005 to 2006 before joining the faculty at UC Berkeley. His research interests focus on next-generation electronic materials and devices.

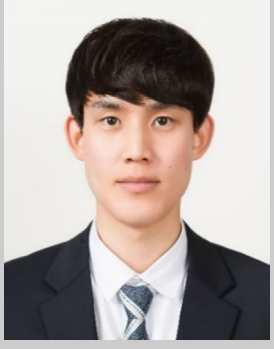

Junseong Ahn is an assistant professor in the Department of Control and Instrumentation Engineering at Korea University. He received his BS, MS, and PhD degrees from Hanyang University (2017), KAIST (2019), and KAIST (2023), respectively. His current research interests include micro/nano structuring and its application to sensors and energy harvesting devices.

© 2025 The Author(s). Advanced Functional Materials published by Wiley-VCH GmbH

16163028, 0, Downloaded from https://advanced.onlinelibrary.wiley.com/doi/10.1002/adfm.202519859 by Inkyu Park - Korea Advanced Institute Of , Wiley Online Library on [10/12/2025]. See the Terms and Conditions (https://onlinelibrary.wiley.com/terms-and-conditions) on Wiley Online Library for rules of use; OA articles are governed by the applicable Creative Commons License

Inkyu Park received his B.S., M.S., and Ph.D. from KAIST (1998), UIUC (2003), and UC Berkeley (2007), respectively, all in mechanical engineering. He has been with the department of mechanical engineering at KAIST since 2009 as a faculty and is currently a full professor, vice department head, and KAIST Endowed Chair Professor. His research interests are nanofabrication, smart sensors for healthcare, environmental and biomedical monitoring, nanomaterial-based sensors, and flexible & wearable electronics. He has published more than 206 international journal articles (SCI indexed) and holds more than 50 registered domestic and international patents in the area of MEMS/NANO engineering.

© 2025 The Author(s). Advanced Functional Materials published by Wiley-VCH GmbH

16163028, 0, Downloaded from https://advanced.onlinelibrary.wiley.com/doi/10.1002/adfm.202519859 by Inkyu Park - Korea Advanced Institute Of , Wiley Online Library on [10/12/2025]. See the Terms and Conditions (https://onlinelibrary.wiley.com/terms-and-conditions) on Wiley Online Library for rules of use; OA articles are governed by the applicable Creative Commons License